NGU
Norges geologiske undersøkelse
Geological Survey of Norway

GEOLOGI FOR SAMFUNNET
GEOLOGY FOR SOCIETY

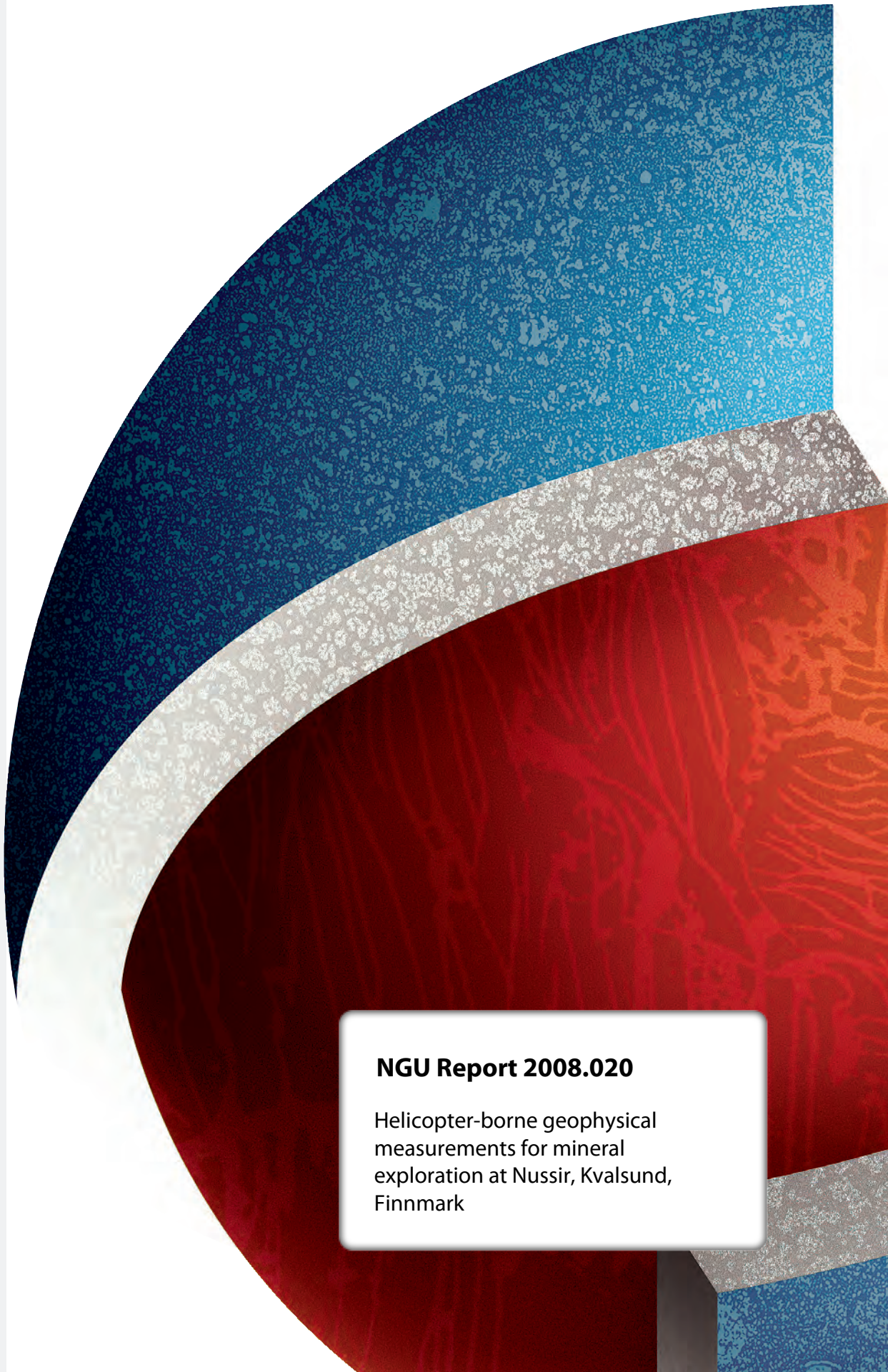

NGU Report 2008.020

Helicopter-borne geophysical measurements for mineral exploration at Nussir, Kvalsund, Finnmark

Geological Survey of Norway
N-7491 TRONDHEIM, Norway
Tlf. +47 73 90 40 00
Telefaks +47 73 92 16 20

REPORT

Report no.: 2008.020 | ISSN 0800-3416 | Grading: Confidential until 01.04.2011

Title:
Helicopter-borne geophysical measurements for mineral exploration at Nussir, Kvalsund, Finnmark.

Authors:
Björn H.Heincke , Janusz Koziel, Peter Walker and Rolf Lynum

Client:
Nussir as

County:
Finnmark

Commune:
Kvalsund

Map-sheet name (M=1:250.000)
Hammerfest

Map-sheet no. and -name (M=1:50.000)
1935 I Repparfjorden

Deposit name and grid-reference:
Nussir, 390500 - 7818100 UTM zone 35

Number of pages: 32 Price (NOK):
Map enclosures: 13

Fieldwork carried out:	Date of report:	Project no.:	Person responsible:
17.10.07 - 15.11.07	12.03.2008	321500	Jan S. Rønning

Summary:
The mining company *Nussir AS* is interested in (re-)evaluating the copper resources in a dolomite layer of the Nussir area in the Kvalsund municipality (Finnmark). To get a better estimate of the extent of this ore deposit and to gain the understanding of the principal geological structure of the region, NGU performed helicopter-borne geophysical measurements (magnetic, frequency-domain EM, spectral gamma ray radiometry) in the Nussir area (size: ~190 km^2) in autumn 2007.

In this report we will present the calibration, acquisition, processing and visualization of all recorded helicopter data sets. During acquisition the crystal for the radiometric measurements was mounted directly at the bottom of the helicopter, whereas the magnetometer and the EM-transmitter and receiver coils (5 frequencies; horizontal coplanar and coaxial oriented) were mounted in a bird hanging 30 m below the helicopter. The helicopter survey comprised 240 lines with a line spacing of 100 m. Average helicopter altitude was 65 m. Processing procedures comprised many of commonly applied filters and corrections. The most critical step in radiometry processing was the removal of air radon counts from the uranium window. The most difficult processing step for the EM was the manual residual drift correction. Final radiometric, magnetic and (both inphase and quadrature) EM data of the three highest frequencies 6606 Hz, 34133 Hz and 7001 Hz have a good data quality. Only the data quality from the two lowest frequencies 880 Hz and 980 Hz suffers from a low signal-to-noise ratio. Large parts of the regions are characterized by "negative" inphase data, typical for regions with high susceptibility and/or high resistivity. All collected data have a significant higher quality and resolution than earlier airborne data collected by the NGU in the same area in the seventieths.

Final processed magnetic data are presented in maps showing the total magnetic field and its first vertical derivative. Final processed radiometric data are presented by potassium, uranium and thorium ground concentration maps and a ternary plot. Final processed EM data are presented in resistivity maps and profile plots showing either apparent conductivities or inphase/quadrature data.

Keywords: Ore	Copper	Geophysics
Helicopter measurements	Magnetic measurements	Electromagnetic measurements
Radiometric measurements		Scientific report

CONTENTS

1. Introduction

Nussir AS and *Wega Mining* contracted NGU to perform helicopter-borne geophysical measurements (magnetic, frequency-domain EM and radiometry) for mineral exploration in two adjacent regions east of the Vargsundet about 25 km south of Hammerfest, Finnmark county. Because of obvious practical aspects both regions were surveyed together and considered as one dataset during processing. However, we will present and describe here only the results from the region that are surveyed on behalf of the *Nussir AS*[1]. *Nussir AS* is interested in (re-) evaluating the copper resources in a dolomite layer of the Nussir area (Kvalsund municipality).

It was assumed that the kind of mineralisation has only weak electric conductivity contrast relative to the surrounding rocks. To evaluate if the associated electric anomaly can be identified by helicopter EM data, the NGU performed 2-D geoelectrical and IP (induced polarisation) test measurements along and across the outcropping deposit in autumn 2007 (Rønning et al., 2007). Resistivities between 50-200 and 1000-10 000 Ωm were determined for the mineralisation and the surrounding rocks, respectively. Results suggested that the deposit layer dips steeply towards north and that the thickness of the mineralisation was ~4 m. Modelling performed by Peter Walker from *Geophysical Algorithms* (Canada) indicates that the electromagnetic response of a such thin structure with a relatively weak electric contrast relative to the surrounding rock is probably only resolvable by the highest frequency (34133 Hz) of the EM Hummingbird system (Rønning et al., 2007) from the NGU.

The mineral bearing layer could not be identified in the EM data from an earlier helicopter geophysical study (magnetic, EM and radiometry) of the NGU in the Repparfjord region (Håbrekke, 1979). However, this system (SANDER type) operated with low frequency of 1000 Hz and was inadequate for mapping such small structures with weak electrical contrasts. Moreover, positioning was highly inaccurate due to the lack of modern GPS systems, such that also magnetic and radiometric data provided reduced detailed information about the structure.

Because of the improvement of geophysical instruments and positioning systems in the past thirty years, the resolution of all three airborne methods is significantly higher nowadays. Accordingly, it was decided to refly this region south of the Vargsundet to re-evaluate the mineral resource potential. A frequency-domain EM system with frequencies ranging from 880 Hz to 34133 Hz was used. Processing of the three highest frequencies had highest priority because the deposit had a low conductance and so was unlikely to be as detectable with the low frequencies. Also magnetic and radiometric measurements were considered as useful in advance: Magnetic data can provide important information about the trend of main structures because rock types in the region show clear variations in their magnetic properties. Radiometry is suited to map natural radionuclide concentrations from the near-surface rocks and accordingly help to refine the existing geologic information because thick soil or sediment coverage exists only locally in this area.

[1] Results from the area around the Ulveryggen are summarized in an own (confidential) report for *Wega Mining*.

This report has its focus on calibration, acquisition, processing and visualization of all recorded helicopter data. Procedures are presented in a way such that the client can better estimate data quality and limitations of the data. In addition, short methodological descriptions of the magnetic, electromagnetic and radiometric methods are presented in Appendix A. An interpretation of the results from the geophysical helicopter data is not provided in this report, but will be presented in a following NGU report from Viola et al., 2008.

2. Equipment

Following equipment was used during the measurements. The equipment was installed in a helicopter owned by the company *HELITEAM* from Harstad/Norway.

2.1 Magnetic

A Scrintex CS-2 cesium magnetometer is located in the EM-bird (sonde). It measures the total magnetic field with a resolution of 0.001 nT. A base station was a Scrintex ENVI proton magnetometer with a resolution 0.1 nT.

2.2 Electromagnetic

A 5-frequency Geotech Hummingbird EM system was used to acquire in-phase and quadrature data. Three of the frequencies (880, 6606 and 34133 Hz) have coils oriented in a horizontal coplanar geometry. The remaining two frequencies (980 and 7001 Hz) are oriented coaxial (see also Appendix B). The coils for the four lower frequencies are separated by ~ 6m. For the coils having with a frequency of 34133 Hz is the separation 4.9 m. The resolution of the system is in the range of 0.1 ppm.

2.3 Radiometry

The radiometric measurements were carried out using a 256 channel GR820 gamma ray spectrometer with sodium iodide detector packs with a total crystal volume of 20.9 l (16.7 l downward and 4.2 l upward directed). Energy from 0.2 MeV until 3 MeV is collected in the channel windows 1-254. Channel 255 (cosmic channel) covers energy above 3 MeV.

2.4 Positioning systems

For the helicopter positioning a GPS system from Seatex (SEAPOS 100E) was used. This system has an accuracy of ±5 m. Moreover, a Bendix/King radar-altimeter was mounted on the helicopter. Its accuracy is 5 % of the measured altitude. The time sampling of the GPS was 1 s.

2.5 Recording system

The recording systenm is an intergrated part of the Hummingbird EM-system.

3. Calibration

The EM system was calibrated in Bymarka site outside of Trondheim by J. Koziel on October 8, 2007. Calibration following the "Hummingbird User Manual" of Geotech Ltd. consists of phasing and calibration with external calibration coil. After the system was turned on and heated for one hour, all five frequencies were initially phased with a ferrite bar. Once the phasing checks were done, the amplitudes were then calibrated on each of the inphase and quadrature channels with external calibrate coil. After transportation to Hammerfest the EM system was turned on and checked on October 15, 2007. In the nights between acquisition days the temperature within the bird was held on a constant level by an internal heating to lessen the drift of the EM backgrounds due to thermal variations at the beginning of the flights.

The radiometric data were only considered as supplement information. Due to the short preparation time, no calibration measurements were possible before this field campaign. Instead stripping factors and sensitivity factors were used that were determined from calibration pad measurements at the NGU by Mark Smethurst (Rønning et al. (2003)).

Most of the calibration routines we perform at the NGU are described in a report from Rønning et al. (2003).

4. Acquisition

The company *HELITEAM* provided the helicopter and pilots for the airborne measurements. Janusz Koziel and Rolf Lynum (both from the NGU) were responsible for the data acquisition. Data from all three methods (gamma ray spectrometry, magnetic and EM) were collected simultaneously. The crystal for the radiometric measurements was mounted directly on the underside of the helicopter, but the magnetometer and the EM-transmitter and receiver coils were mounted in the bird hanging 30 m below the helicopter during the flights (see Figure 1). The GPS system was used for positioning and the radar altimeter was used to determine height above surface topography (STP).

Figure 1: Photo from the measurements in the Finmark.

The company *HELITEAM* from Harstad/Norway provided the helicopter (AS 350 B3) and pilots for the airborne measurements. The helicopter was stationed on the Hammerfest airport and all flights started and ended there. The field campaign lasts from the 17.10.07 until 15.11.07, however, due to bad weather conditions and limited accessibility of the area (reindeer herd) measurements were only performed on 11 days (see Figure 2). The surveyed region has a size of about 190 km^2**,** but only 84 % of the complete survey is presented in this report (see Figure 3). The remaining part around the Ulveryggen is presented in the report for *Wega Mining*. To ensure a uniform and dense data coverage for all methods, the measurements were performed along 240 northeast-southwest directed, parallel lines with a narrow line spacing of 100 m (see Figure 3). In the following we will name the most eastern line as L1 and the most western line as L240. In addition, four tie-lines (spacing 2.5 km) were flown perpendicular to the general line direction. The average flying altitude during the flight lines was 65 m (resulting in an average bird height of 35 m) and the average speed was 70 km/h. However, due to the relatively strong topography variations (0 - 710 m above sea-level) it was not always possible to keep the speed and flying altitude constant.

Figure 2: Photo from the helicopter during surveying (25.10.2007). Most of the area is covered by a thin layer of snow.

After every fourth flight line and at the beginning/end of each flight so-called background calibration tests were performed that were required in the EM processing to remove drifts in the EM data (see EM processing section). For this purpose the helicopter was flown up to an altitude (above topography) of about 1200 feet (~ 365 m). At this high altitude the ground response is negligible, so the secondary field should be close to zero and the remaining level is associated with the actual drift. To ensure that highly conductive seawater had no effect, background calibration flights were performed always above land.
For aircraft and cosmic correction in the radiometric data (see processing section) calibrations flight were performed with varying altitudes above water (some kilometres distanced from land).

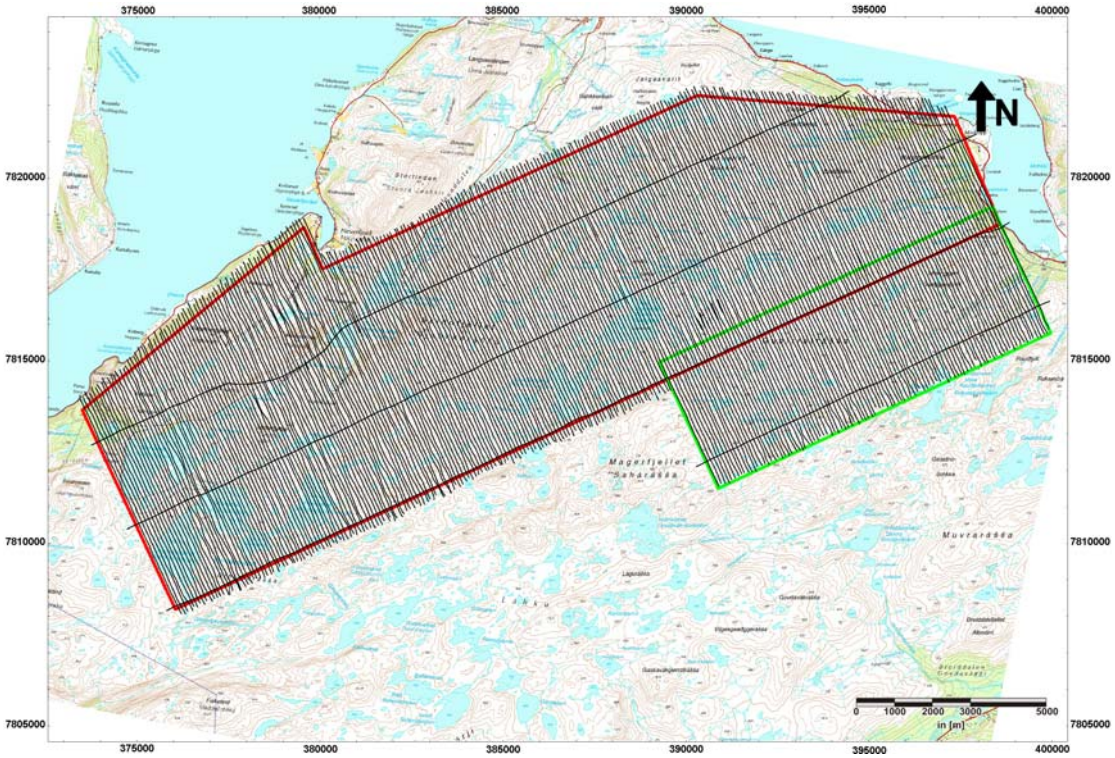

Figure 3: Region south of Repparfjord/Finmark. The black lines indicate the flight and tie lines of the helicopter survey. Regions surrounded by red and green lines were surveyed for the client *Nussir AS* and *Wega Mining*, respectively.

Low mean HDOP[2] values of < 1 for the GPS data indicate that very good satellite coverage existed during measurements usually resulting in a spatial resolution of few meters. For magnetic and electromagnetic measurements ten samples per second were recorded resulting in a data spacing of about 2 m during data acquisition. For radiometry a recording time of 1 s for each measurement was chosen that can be considered as a compromise to get both an acceptable measuring interval of about 20 m and enough counts to get representative spectra. Referring to a formula given by Grasty (1987), we expect that about eighty percent of the gamma ray counts for a single measurement come from an area on the ground with a radius 110 m (assuming a height of 65 m and no movements). This value can be considered as an estimate for the spatial resolution of the radiometric measurements.
For removal of the diurnal magnetic field variation, a stationary magnetometer was placed on the airport in Hammerfest about 25 km from the survey area and recorded a sample every 3 seconds.

5. Processing

For most processing staged the commercial Oasis Montaj software "Geosoft" was used (Oasis Montaj Geosoft, 2007). However, some of the more advanced processing

[2] HDOP (Horizontal Dilution Of Precision) is a measure describing the effects of the satellite geometry onto the horizontal resolution of the GPS. Values smaller than 4 are associated with very good satellite coverage (see e.g.: http://www.kowoma.de/gps/Fehlerquellen.htm).

steps (e.g. micro-levelling, NASVD, spectral-ratio method and topographic corrections) were conducted with in-house software.

5.1 Magnetic data

The bird is usually not located directly below, but some meters behind the helicopter during acquisition. Because the GPS was fixed at the helicopter the magnetic data have to be lag-corrected (or parallax corrected). A shift of four fiducials corresponding to about 8 m in flight direction was used as correction.
To correct for diurnal variations of the external magnetic field a spiking and low-pass filtered version of the total magnetic field from the base station was subtracted (and an average regional field of 53400 nT added[3]). After this procedure a low pass filter was applied to eliminate spikes and noise bursts from the data. Tie lines were used to check the consistency of the data level of all flight lines. Residual line-level errors – remaining inconsistencies between adjacent flight lines – were removed by passing a median filter-based micro-levelling method (see Figure 4) over the dataset (Mauring and Kihle, 2006). A flow path of the magnetic data processing (including the used parameters) is given in Appendix C1. An overview about standard processing of airborne magnetic data is given e.g. by Luyendyk (1997).

Specific comments:
Because of the partly strong topography over parts of the surveyed region, the speed of the helicopter and the horizontal offset of helicopter and bird varied. Therefore a fixed lag-correction was imperfect in some parts of the survey. For all measuring days no significant high frequency noise was observed in the data from the magnetic base station. No significant discrepancies in the data level of the flight lines were found by considering tie-line data. Finally processed magnetic data had a good quality.

[3] Because this is a relatively small survey, we can assume that the regional field is constant and we did not conducted an IGRF (International Geomagnetic Reference Field)-correction.

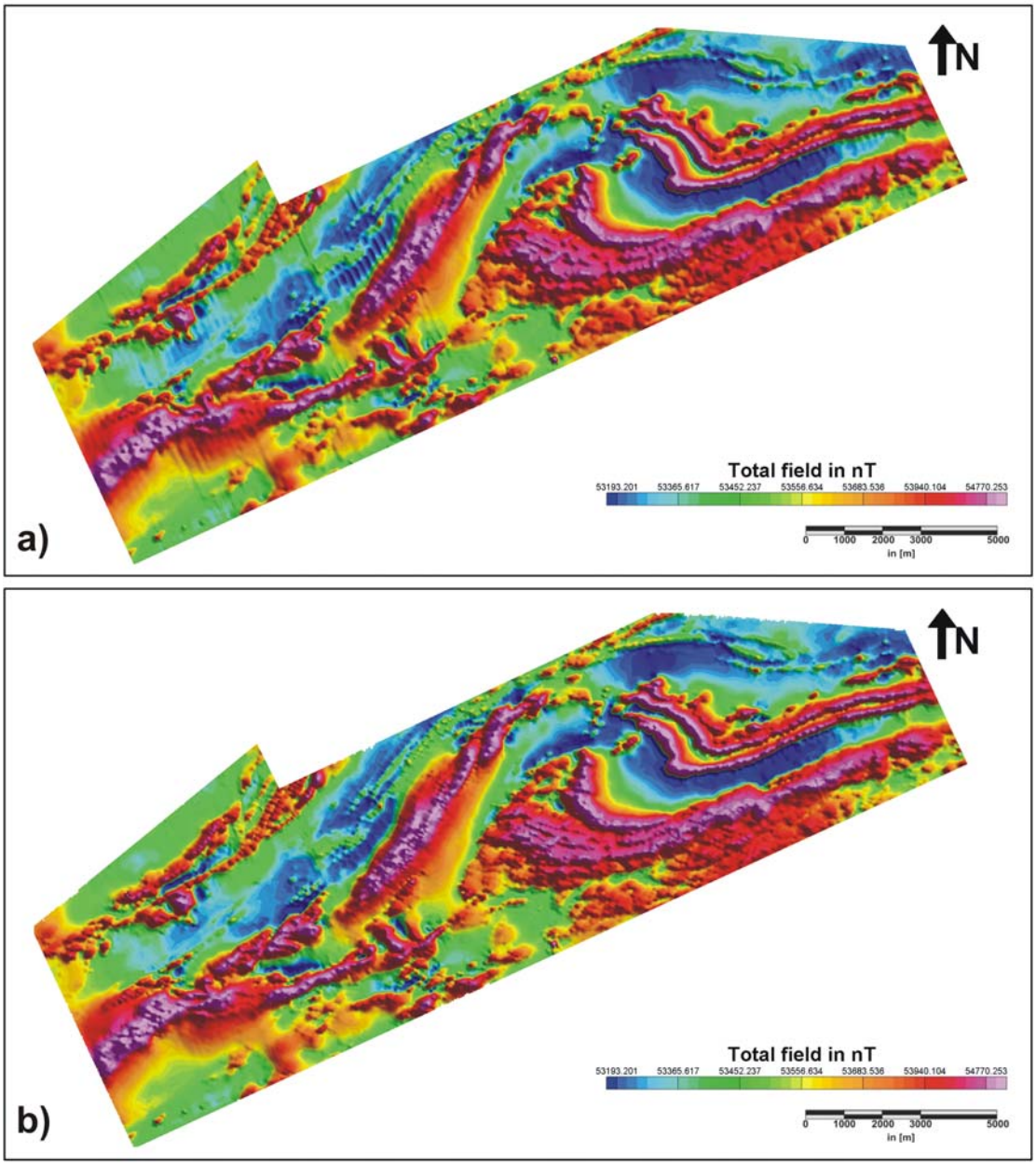

Figure 4: Shaded map showing the total magnetic field a) before and b) after applying the micro-levelling filter. Artificial strips parallel to the flight lines are significantly removed.

5.2 Electromagnetic data

During processing the secondary field data from the in-phase (real) and the quadrature (imaginary) part were considered separately for each frequency. However, the processing procedure for all resulting 10 datasets was similar.

As was done for the magnetic data, a lag correction was performed. A non-linear low-pass filter was applied accounting for removal of spikes and other high-frequency spurious noise (Naudy and Dreyer, 1968). The by far most time consuming and challenging part in HEM data processing was the removal of a time variant drift ("drift correction" or "levelling") that was different for all frequencies. In order to remove this drift, mean values from the background tests (see Figure 5) were

calculated and tabulated together with their corresponding (mean) recording times. By means of linear interpolation with time across the whole dataset, a drift estimate was obtained for every data point. "Zero levels" adjustment was then achieved by subtracting the drift estimates from the data (Valleau, 2000).

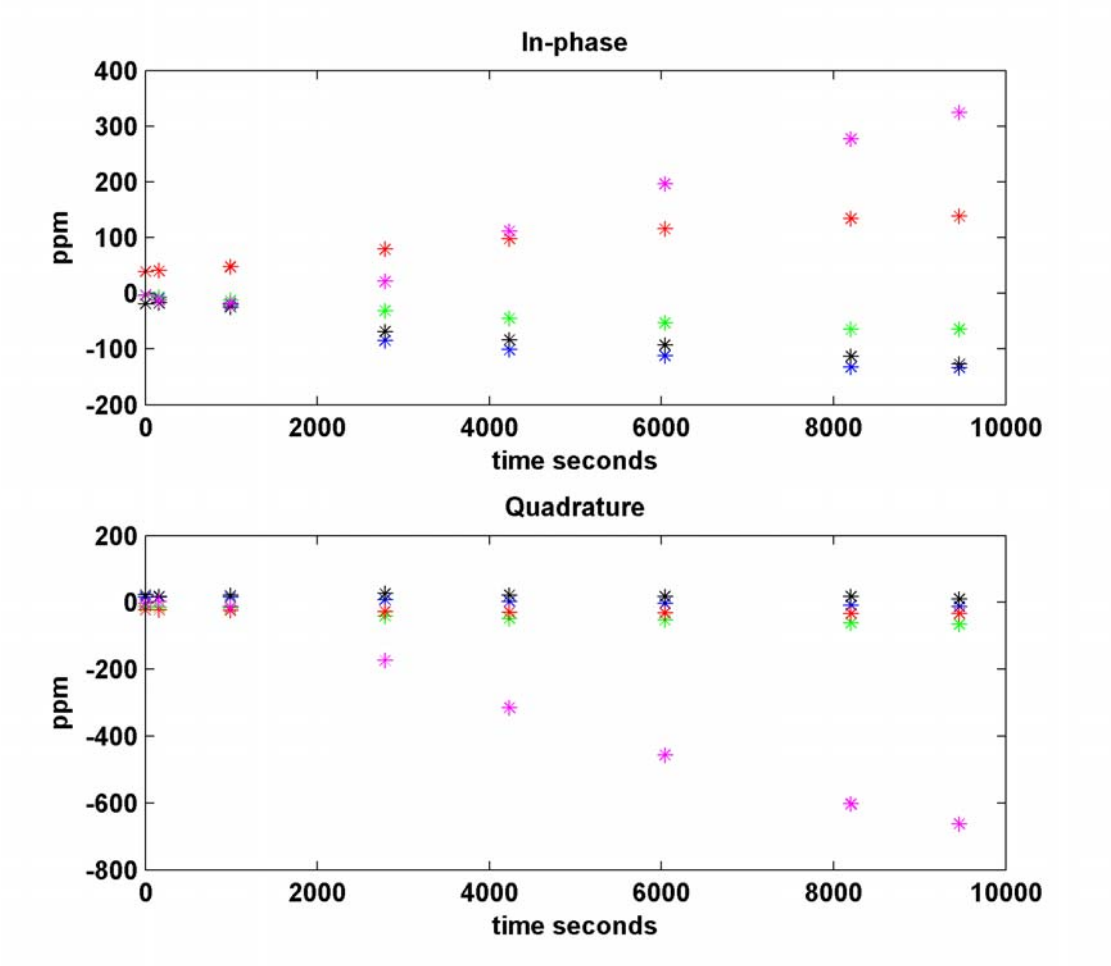

Figure 5: Mean values obtained from background tests of the 16th flight (15.11.2007). The drift of the frequencies 880Hz, 980Hz, 6606Hz, 7001Hz and 34133Hz are shown with black, green, red, blue and magenta stars, respectively.

Unfortunately, the drift often did not vary linearly with time. This resulted in residual errors after the automated drift correction and manual re-levelling was required for all data sets. The manual drift correction was not directly performed on the inphase and quadrature data, because amplitude levels of the secondary field are also strongly dependent on the source distances and hence on the flight heights. To account for this, inphase and/or quadrature data were transferred by a non-linear inversion procedure to apparent resistivities values. Because the effect of the bird height is considered in the inversion algorithms, variations of the resistivity level in adjacent lines could directly be associated with levelling errors in the corresponding inphase and/or quadrature data. To remove the residual drift errors, inphase and/or quadrature data were adjusted in several iterations until the apparent resistivity level of adjacent lines were similar. Finally, the same micro-levelling algorithms like for the magnetic and radiometric data was applied to the apparent resistivity data (Mauring and Kihle, 2006). A flow path of the EM processing is given in Appendix C2.

The inversion algorithm is described in the manual of the GEOSOFT software and forward equations are described in the book from Wait (1982). An overview about processing of helicopter EM-data is given for example by Valleau (2000).

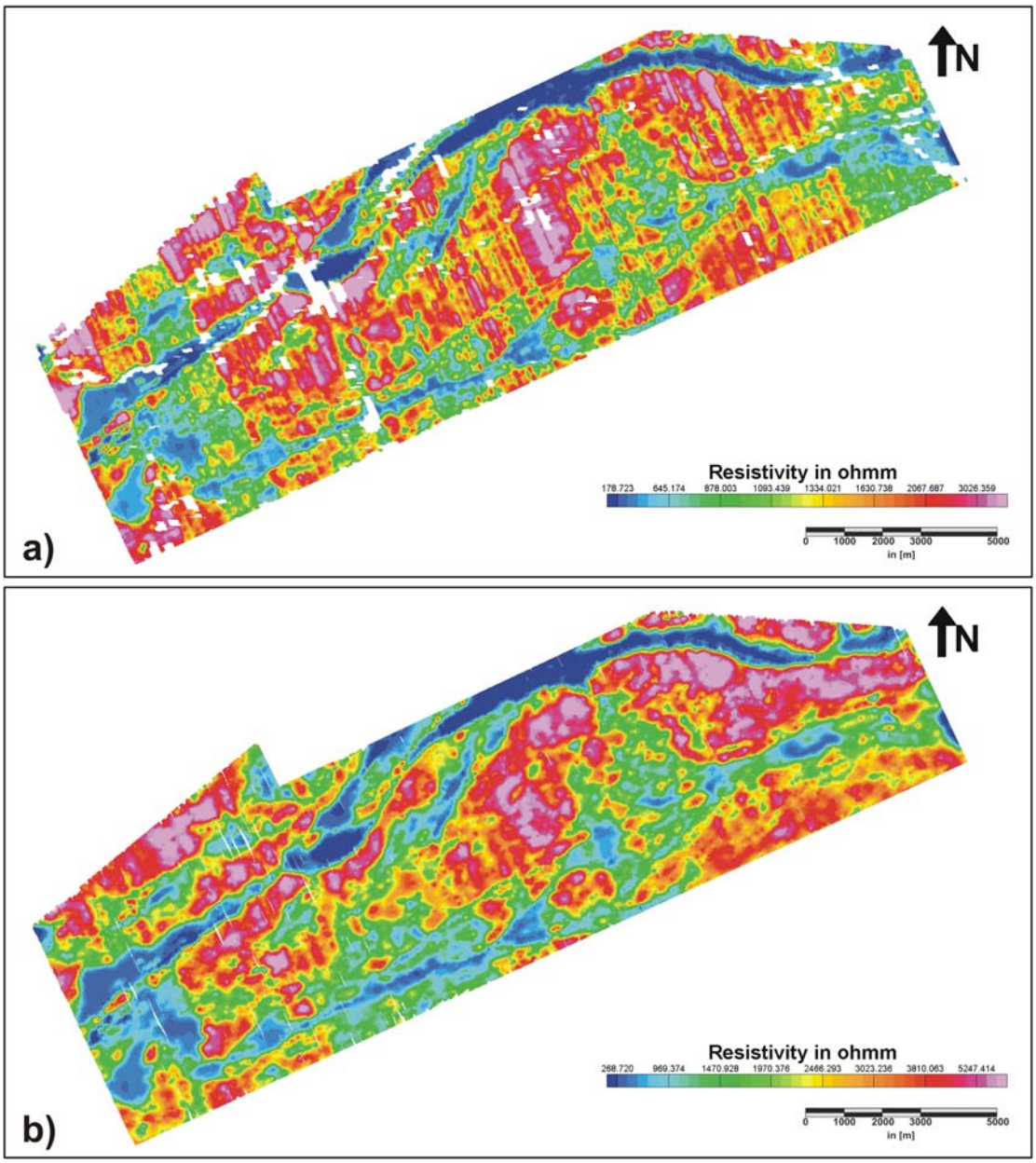

Figure 6: Map of apparent resistivity from the quadrature term of the coaxial 7001 Hz frequency. Figures a) and b) show apparent resistivity values with and without applying manual drift-correction (and micro-levelling).

Specific comments:

For two flights the 880 Hz horizontal coplanar- data were distorted in an irreparable way due to electronic problems of the EM system. The data of the corresponding flight lines L146-L166 and L190-L205 have not been processed (see Figure D- 5).

Due to strong topographic variations in the surveyed region it was challenging for the pilot to keep the bird always at low height above the topography. Because the recorded secondary EM signal decreases rapidly with increasing flight height (with

about z^{-3}), data were considered as unreliable in regions where the bird-height exceeded 45 m. These data were therefore removed during processing.
In some high resistive parts of our surveyed region the impact of the magnetic susceptibility was so significant that the inphase signal was negative. Since the inversion assumes free-space susceptibility, inphase data from these areas could not be inverted for apparent resistivity. Large regions with such negative apparent resistivities appeared for the two lowest frequencies (880 and 980 Hz), so we decided to present the quadrature and inphase data instead of the corresponding apparent resistivities for these two frequencies. A distinct correlation of the magnetic anomalies with differences in apparent resistivities from inphase and quadrature data (of the higher frequencies) confirms that the reduction of apparent resistivities from inphase data is caused by magnetic susceptibility.
Average noise level was 1-2 ppm for most of the data and little spheric activity was observed. However, along the power line that crosses the survey area in the north-eastern part of the survey some noise is visible in data from the two lowest frequencies (see Figure D- 5 and D-6).
Data from the higher frequencies are more reliable due to their higher average amplitude level than the data from lower frequencies. For lower frequencies (in particular for the 980 Hz coaxial configuration) it was therefore challenging to perform a satisfying manual drift correction. However, these are inherent limits of the EM frequency-domain method that have been known in forehand.
Considering the limitations of the EM method, the final data quality was good for the three higher frequencies. The data quality from the two lower frequencies suffers to a certain extent from a low signal-to-noise ratio.

5.3 Radiometric data

Processing of the airborne gamma ray spectrometry data began with noise reduction of full spectrum data using the clustered NASVD method (Minty and McFadden, 1998). Spectral windows were then live time corrected and aircraft and cosmic background values eliminated (e.g. IAEA, 2003). The spectral-ratio method of Minty (1998) was applied to remove the effects of radon in the air below and around the helicopter. Window stripping was used to isolate count rates from the individual radionuclides K, U and Th (IAEA, 2003). The topography in parts of the measured region is rough and stripped window count rates were corrected both for variations in ground clearance and ground geometry (Schwarz et al, 1992). As was done for the magnetic and EM data, a micro-levelling was performed for all windows (Mauring and Kihle, 2006). Finally, radionuclide count rates were converted to effective ground element concentrations using calibration values derived from calibration pads at the Geological Survey of Norway in Trondheim. A list of the used parameters in the processing scheme is given in Appendix C3.
For further reading standard processing of airborne radiometric data we recommend the publication from Minty et al. (1997).

Specific comments:
Gamma radiation from the ground is significantly attenuated at relative high flight altitude of ~65 m and relatively small counts rates are detected from the crystal[4].

[4] A larger crystal volume would increase the count rates. However, weight restrictions of the helicopter limit the size of the crystal volume.

Therefore the signal-to-noise ratio of the raw data was, in particular, for the uranium and thorium window poor. However, the applied noise reduction routine (clustered NASVD; see Minty and McFadden, 1998) was able to reduce most of the stochastic noise without removing significantly real features. After noise reduction the quality for all three energy windows was good (see Figure 7).

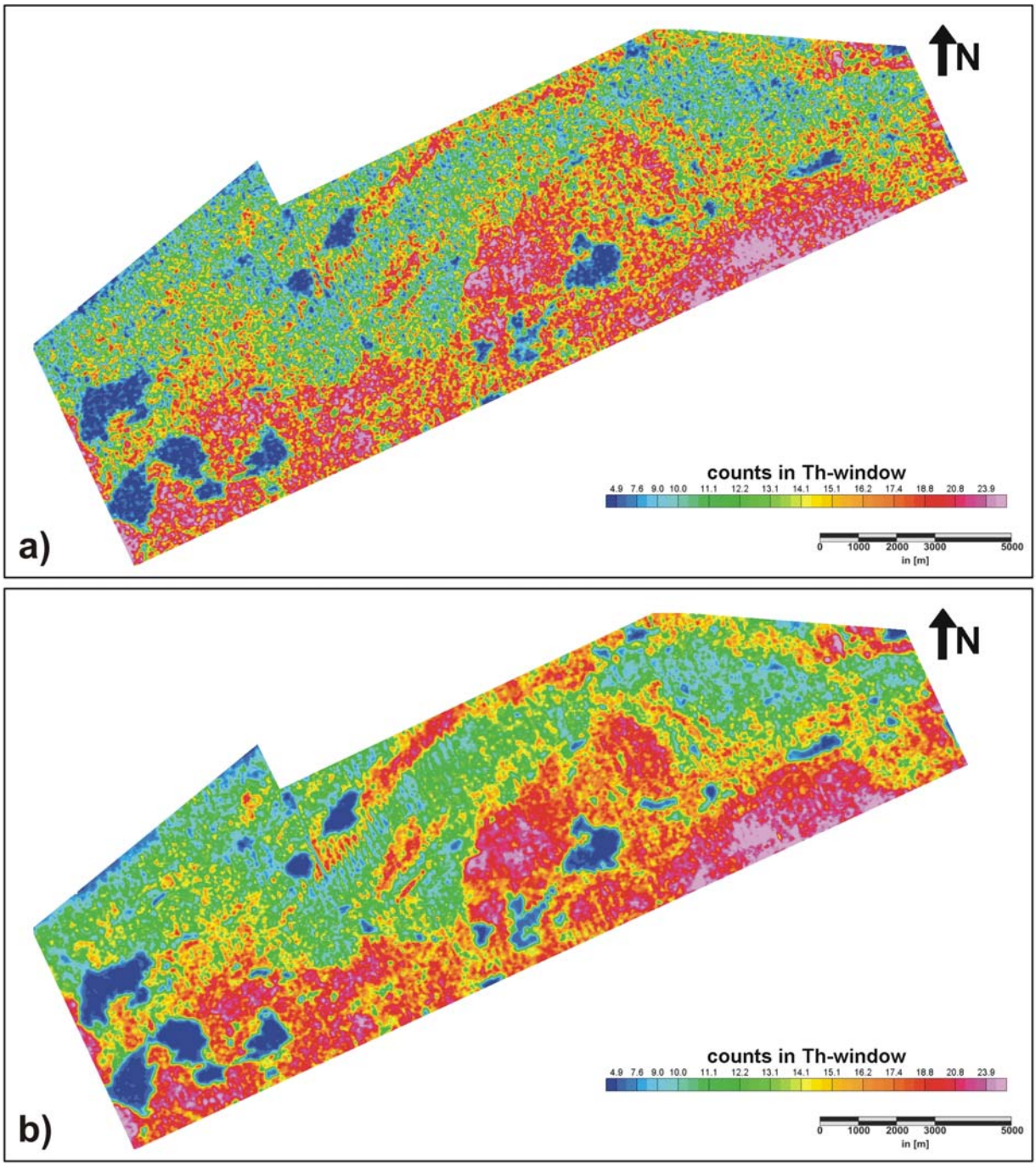

Figure 7: Map showing counts in the thorium window a) before and b) after applying a clustered NASVD. By this processing step random noise is significantly removed and real features become more pronounced.

Airborne radiometric investigations are usually performed during periods with dry and constant weather conditions because water-saturated soil or snow can significantly reduce the radiation from the ground beneath and rain, wind direction

and strength are all factors governing the concentration of air radon. Our measurements were carried out in a period with unstable weather conditions responsible for variable snow coverage in large parts of the surveyed regions during most of the time of the acquisition period. Despite these rather improper conditions we found no indication in the data that moisture or snow coverage noticeably attenuated the gamma radiation from the ground. However, air radon concentrations changed strongly from day to day (see Figure 8), and for some flights the counts rates from radon were in average approximately a factor 3 higher than the actual counts from the uranium. This made reduction of radon in the uranium window to the most critical and challenging step in radiometry processing. However, final results show that the applied spectral ratio method (Minty, 1998) was able to remove successfully mostly all counts from air radon in the uranium window (Figure 8).
Final concentrations determined from flight lines and tie lines at intersection points show no significant differences. This indicates that applied processing was adequate for all count windows.

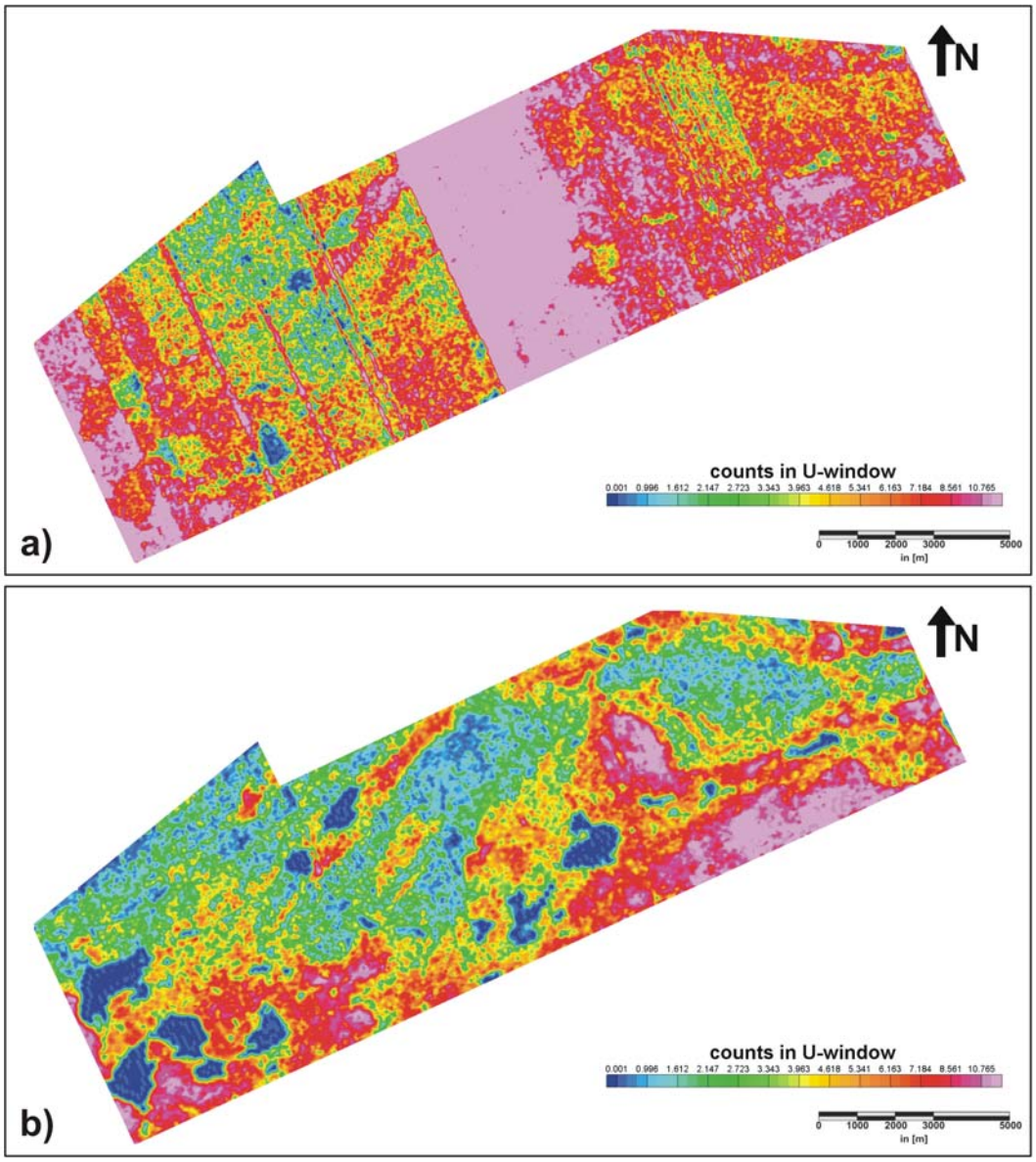

Figure 8: Map showing counts in the uranium window a) before and b) after removing air radon counts and applying topographic correction.

6. Final data

Final data are presented either as grids (using minimum curvature gridding) or as profile plots. Some of the grids are colour-shaded such that small and/or elongated features can be better seen in the plot. The gridded data have a sampling rate of 40 m in both x and y direction. Finer sampling was not used because alias artefacts appeared in test plots with finer sampling intervals. In the profile plots parameters (e.g. inphase and quadrature term or final conductivities) are plotted as traces along the flight lines.

6.1. Magnetic data

The total magnetic field in nanoteslas (abbreviated nT) and its first vertical derivative in nT/m are plotted in Figure D- 1 and in Figure D- 2. The computation of the vertical derivatives is analogous to the applications of a high-pass filter and suppresses the effect from the regional field while emphasizing near surface effects. Smaller features are therefore often easier identifiable than by original total field maps. If we compare the results from the recent magnetic measurements with the ones from 1977 (Håbrekke, 1979), we see enormous improvements in data quality (see Figure 9). Particularly, navigation related errors are significantly reduced by the usage of GPS positions. But also currently used cesium magnetometers have a significantly higher resolution and processing is more advanced (e.g. levelling procedures).
For further reading about visualisation techniques in magnetic mapping, we recommend the paper from Gunn et al.(1997).

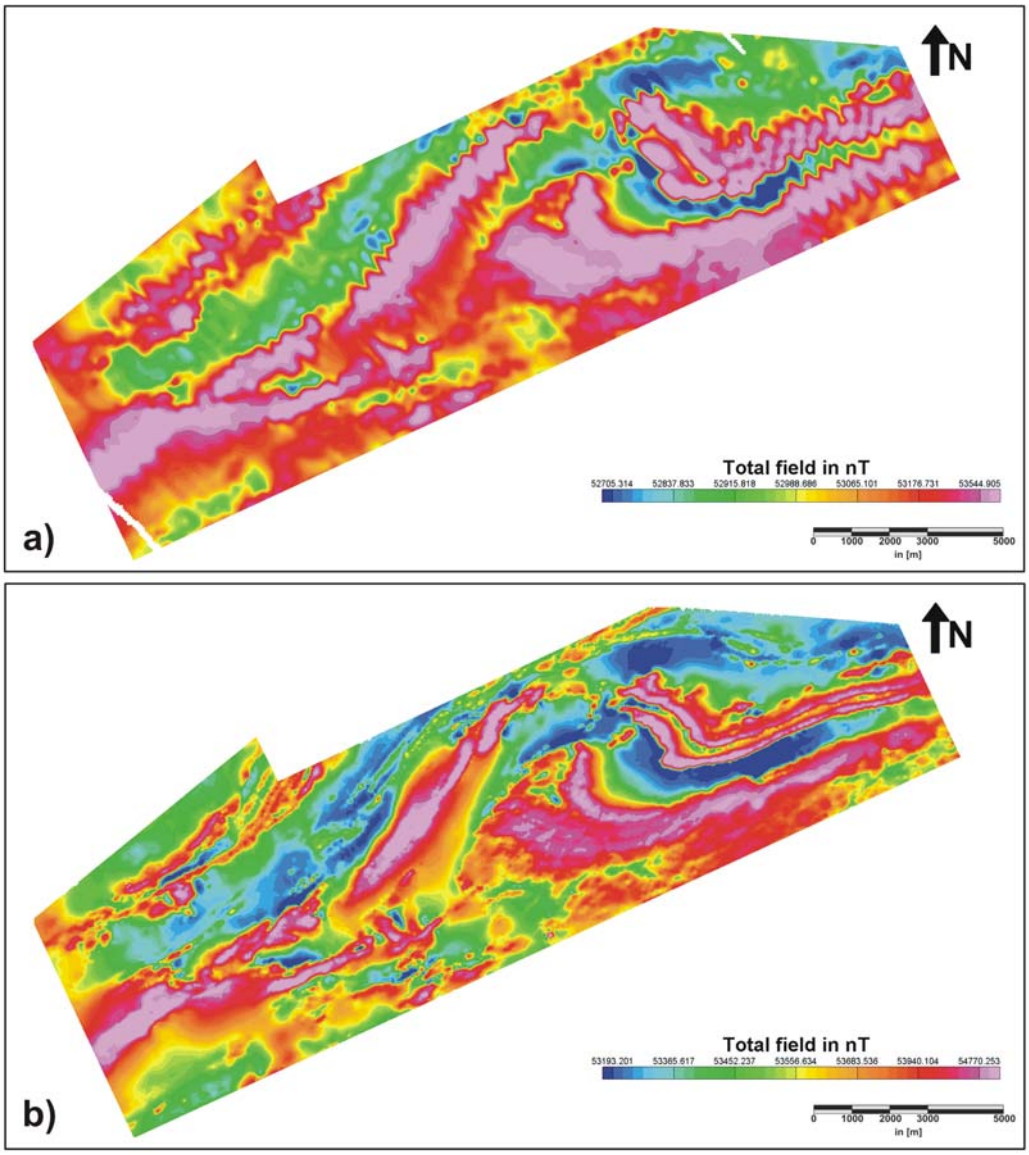

Figure 9: a) Magnetic total field determined from a former airborne survey in 1977. b) Magnetic total field determined from our helicopter survey from 2007.

6.2. Electromagnetic data

Results from the electromagnetic data are presented in Figure D- 3 to Figure D- 9. Apparent resistivities of the quadrature data from the frequencies 7001 and 34133 Hz are presented in Ωm as gridded data in Figure D- 3 and Figure D- 4. The profile plots in the Figure D- 7 to Figure D- 9 show apparent conductivities in S/m. Apparent conductivity, the inverse of apparent resistivity, was chosen as unit, because structures with increased conductivity (more likely related to ore deposits) are more easily to identify. Profiles from apparent conductivities from inphase data are plotted on top of apparent conductivities from quadrature data. In this way also regions with induced magnetic affects are highlighted because the conductivity values from the inphase data become weaker or are even vanishing. The profile plots in Figure D- 5 and Figure D- 6 show inphase and quadrature data from the lowest frequencies 880 and 980 Hz. The negative and positive parts of the inphase and quadrature data are

highlighted, respectively, and in this way both more conductive regions and regions with higher magnetic susceptibility are emphasized.

6.3. Radiometric data

Maps with K, U and Th concentrations obtained from processed radiometry data are shown in to Figure D- 10 to D-12. Effective potassium concentrations are given in % and effective uranium and thorium concentrations in ppm. The total counts after processing are presented in Figure 10. In a first order the ground concentrations of all three radioelements correlate with each other. Such a rough first-order correlation of thorium and uranium nuclides is typical for many rocktypes (IAEA, 2003). Moreover, moisture in the ground/soil has a significant attenuating effect onto the gamma radiation from all three radioelements and lakes are clearly visible in radiometry maps by showing no gamma radiation.

To better image relative relationships of K, U and Th so-called ternary radioelement maps are used. A ternary radioelement map is a colour composite image generated by modulating the red, green and blue phosphors (RGB image) or yellow, magenta and cyan dyes (CMY image) in proportion to the radioelement concentration values of K, U and Th. In Figure D- 13 a RGB ternary plot (red = potassium; green = uranium and blue= thorium) with histogram scaled colour coding is shown.

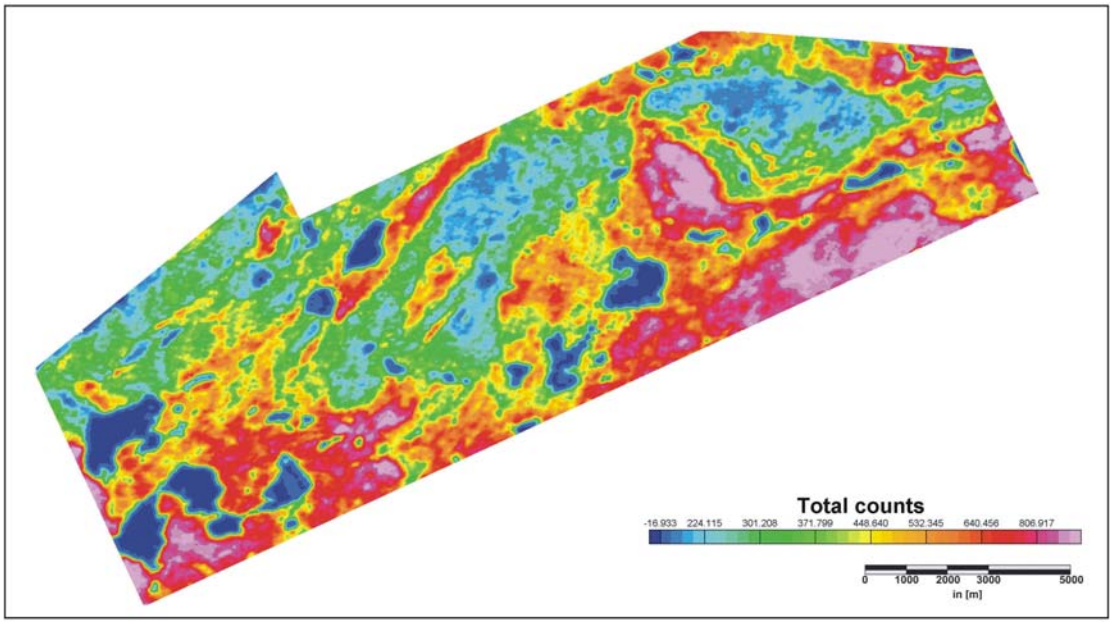

Figure 10: Number of total counts after radiometry processing.

7. Literature

Fitterman, D.V. and Labson, V.F. (2005). Electromagnetic induction methods for environmental problems. In: *Near Surface Geophysics.* Editor: D.K.Butler. Society of Geophysics (SEG). pp 301-356.

Gunn, P.J., Maidment, D. and Milligan, P.R. 1997. Interpreting aeromagnetic data in areas of limited outcrop. *AGSO – Journal of Australian Geology & Geophysics*, 17(2), 175-185.

Grasty, R.L. 1987. The design, construction and application of airborne gamma-ray spectrometer calibration pads – Thailand. *Geological Survey of Canada*. Paper 87-10. 34 pp.

Håbrekke, H. 1979. Magnetiske, elektromagnetiske og radiometriske målinger fra helikopter over Komagfjordvinduet, Alta og Kvalsund, Finmark. *NGU report 1593 (I-III).*

IAEA**.** 2003. Guidelines for radioelement mapping using gamma ray spectrometry data. *IAEA-TECDOC-1363*, Vienna, Austria. 173 pp.

Luyendyk, A.P.J. 1997. Processing of airborne magnetic data. *AGSO – Journal of Australian Geology & Geophysics.* 17(2). 31-38.

Mauring, E. and Kihle, O. 2006. Levelling aerogeophysical data using a moving differential median filter. *Geophysics,* 71, L5-L11.

Minty, B.R.S., Luyendyk, A.P.J. and Brodie, R.C. 1997. Calibration and data processing for gamma-ray spectrometry. *AGSO – Journal of Australian Geology & Geophysics.* 17(2). 51-62.

Minty, B.R.S. 1998. Multichannel models for the estimation of radon background in airborne gamma-ray spectrometry. *Geophysics,* 63, 1986 - 1996.

Minty, B.R.S. and McFadden, P, 1998. Improved NASVD smoothing of airborne gamma-ray-spectra. *Exploration Geophysics*. 29. 516-523.

Naudy, H. and Dreyer, H. 1968. Non-linear filtering applied to aeromagnetic profiles. Geophysical Prospecting. 16(2). 171-178.

Oasis Montaj Geosoft. 2007. Quick start tutorial – Mapping and processing system. (PDF-download of tutorial is available on webpage: http://www.geosoft.com/resources/tutorials/).

Palacky, G. J. and West, G.F. 1991.Airborne electromagnetic methods. In: *Electromagnetic methods in applied geophysics*. Editor: M.N.Nabighian. Volume 2, Application, Part A and B. Society of Geophysics (SEG). pp 811-879.

Rønning, J.S., Kihle, O., Mogaard, J.O., Walker, P., Shomali, H., Hagthorpe, P., Byström, S., Lindberg, H. and Thunehed, H. 2003. Forsmark site investigation – Helicopter borne geophysics at Forsmark, Ôsthammar, Sweden. *SKB report P-03-41.* 137 pp.

Rønning, J.S., Dalsegg, E. and Walker, P. 2007. Vurdering av helikoptergeofysikk over Nussirforekomsten, Kvalsund kommune i Finnmark. *NGU report 2007.060.* (confidential).

Schwarz, G.F., Klingele, E.E. and Rybach, L. 1992. How to handle rugged topography in airborne gamma-ray spectrometry surveys. *First Break*, 10, 11 - 17.

Valleau, N.C. 2000. HEM data processing - a practical overview. *Exploration Geophysics*, 31, 584-594.

Viola, G., Sandstad, J. S., Nilsson L.P. and Heincke B. 2008. Structural and ore geological studies in the northwestern part of the Repparfjord Window, Kvalsund, Finnmark, Norway.. *NGU report* 2008.029 (confidential).

Wait, J.R. 1982. *Geo-elektromagnetism*. Academic Press, New York. pp.268.

Appendix A: Short description of the methods

Magnetic:

Airborne magnetometry is an efficient method to determine main geological near surface structures and lineaments provided that the associated rock types have measurable magnetic properties[5]. Although magnetic field is a vector field, essentially all modern instruments in common use measure only the total magnetic field. Local magnetic anomalies related to the magnitization of near-surface rock types are superimposed by the much larger main earth fields (~ 53400 nT in the Finnmark), other more regional anomalies and time-variation external fields (usually in the range of ~ 60 nT). The main earth magnetic field has very large wavelength and can be considered as constant for more local studies like the Repparfjord. Also more regional anomalies have larger wavelengths and their influence can be reduced by filtering the data to reduce regional effects. A typical way to do this is to use the vertical derivatives of the magnetic total field for interpretation instead of the total magnetic field itself. The so-called diurnal magnetic field is mainly caused by the interaction of charged particles emitted from the sun with the geomagnetic field. By using a magnetic base station that is situated close to the surveyed region the effect of this slowly varying external field (from minutes to 24 h periods) can be measured and removed from the magnetic helicopter data. However, in some periods occur so-called magnetic storms that are responsible for strong high-frequency magnetic noise that is difficult to remove using base station corrections. Magnetic surveying should not be carried out during these periods.

Electromagnetic:

Airborne EM methods are well-established geophysical methods to determine conductive structures in the subsurface and are very popular in mineral explorations, because many ore deposits, particularly sulfides, are characterized by increased conductivities. Thus, EM systems are capable of directly detecting conductive ore. However, conductivity variations are also present due to the variation in water content of rock, and due to the effects of alteration (silisic alteration would create a resistivity high, whereas sericitic and potassic alteration would create a resistivity low).

Frequency-domain EM systems[6], of the type used in this survey, consist of one or several sets of transmitter and receiver coils that are fixed[7] directly to so-called bird towed from the helicopter. For frequency-domain systems each transmitter coil generates a sinusoidal electromagnetic field. These primary fields induce currents in

[5]The local magnetic field of rocks is typically sensitive to the magnetite content. Therefore classification based on magnetic anomalies varies from other geological classification methods which are often silica based.

[6]In addition to frequency domain systems also time-domain systems (TEM) exist for airborne investigations. Such time-domain systems generate short-term pulses and use the decay characteristics of the secondary field to determine conductivity distributions in the ground.

[7]The advantage of fixing the coils is that the transmitted primary field has always a constant amplitude at the receiver, and thus can be accurately removed from the secondary fields scattered by the earth. Since the primary field is by definition in-phase, fixing the coils means that the in-phase component of the transmitted field can be accurately removed from the in-phase component of the total field measured at the receiver. This in turn means that the in-phase component of the scattered field from the ground can be accurately determined. This is not the case for systems where the transmitter and receiver geometry is not fixed.

conductive underground structures producing time-invariant secondary magnetic fields. In turn these secondary magnetic fields induce a current in the corresponding receiver coils. Because different discrete frequencies and geometric configurations (e.g. horizontal coplanar = both coils are parallel to the horizontal; coaxial = both coils are orientated normal to the flight direction) are sensitive to other conductivities ranges and geometric characteristics of subsurface, helicopter EM frequency systems have several different coil sets. The coaxial sets tend to couple better with vertical structures, while the horizontal coils couple better with flat-lying structures.

To calculate the apparent conductivities (resistivities) in the ground, amplitudes of the inphase (real) and/or quadrature (imaginary) part of the secondary signals are used either in a lookup table method or in an iterative inversion procedure. In this survey, the inversion method was used. Thereby, "apparent" means that the used forward model is based on homogenous half-space assumption and only one conductivity value is calculated for each data point. In this context it is important to note that in-phase amplitudes are not only dependent on conductivities (resistivities), but also on magnetic susceptibility in the near-surface ground. Magnetic susceptibility reduces the inphase amplitudes such that lower apparent resistivities values are obtained from inversion of the in-phase than from inversion of the corresponding quadrature channels in magnetic regions[8].

During measurements not only the secondary field, but also the primary field is detected from the receiver. This primary field is several decades larger due to the short distance from the transmitter coil and have to be reduced during operation. The NGU system uses so-called "bucking coils" (located close to the transmitter coils) to remove much of the signal from primary field in the receiver coils. However, attenuation of the primary field is not perfect and therefore specific calibrations routines ("nulling" and "phasing") are performed before each field campaign.

Small changes in the transmitter-bucking–receiver coil geometry, as well as changes in the electrical properties of the coils and amplifiers in the receiver-bucking coil circuit introduces a slowly varying background drift signal that overprints the secondary field from the ground. This drift must be removed in processing before the secondary field can be used to compute an apparent resistivity. Removal of such a drift is the by far most time-consuming and challenging part of the processing.

Small signal amplitudes close to the noise level provide less reliable apparent resistivity estimates. Therefore, low amplitude inphase/quadrature data should be considered carefully. Amplitude level of inphase/quadrature data are governed by several factors:

- Amplitude level increases with conductivity both for inphase and quadrature data as long as the conductivities are not particularly high. This means more resistive structures are more difficult to identify from EM data.
- Inphase data can be negative where the ground is resistive and magnetic.
- Horizontal coplanar configuration is more sensitive to horizontal structures and its data have usually larger amplitudes than the ones from the coaxial configuration.

[8]Only the induced but **not** the remanent magnetization has an effect onto the inphase amplitude.

- For structures with conductivities typical for many rock types signals from higher frequencies have larger amplitudes than the ones from lower frequencies.

Basic principles of airborne and helicopter borne EM methods are described by e.g. Palacky and West (1991). One among many other recent reviews about EM methods is presented by Fitterman and Labson (2005).

Radiometry:

Airborne gamma ray spectrometry allows mapping of the near-surface concentration of the isotopes thorium-232, uranium-238 and potassium-40, whose decay series (decay) are responsible for mostly all radioactivity from natural sources. ^{40}K has only one daughterproduct (^{40}Ar), but ^{238}U and ^{232}Th decays in a series of 18 and 11 daughter isotopes until the stable isotopes ^{206}Pb and ^{208}Pb are reached. Every product in the decay series has its own specific alpha, beta and/or gamma radiation, leading to characteristic gamma ray energy spectra for ^{40}K and the decay series of ^{238}U and ^{232}Th.

During measurements the gamma spectrum is recorded by a scintillation detector and arranged in 256 equally sized energy channels. In the processing it is possible to separate the contribution of the K, U and Th from the total spectra by using the gamma ray counts in windows around the most significant energy maxima of the decay series. For uranium and thorium series the maxima from the daughter products ^{214}Bi and ^{208}Tl are used. The counts in these windows represent the uranium and thorium ground concentrations assuming that the products in the decay series are in equilibrium (it is assumed that no products are depleted or added)[9]. For determining potassium ground concentrations counts in a window around the ^{40}K peak are used.

Gamma radiation is strongly attenuated by material and therefore only the gamma radiation from the upper 1-2 meters of the subsurface is recorded by helicopter-borne gamma ray spectrometry. This means that information from gamma ray spectrometry is always limited to the shallow features. Soil and drift sediments (but also high water concentrations in the shallow ground) can significantly attenuate gamma radiation from underlying rock. However, in region with no or thin overburden radiometry data can often provide accurate "geological maps", because uranium, thorium and potassium concentrations are closely linked to individual rock types and their origin/development. Because the number of radiometric counts from surface material decreases exponential with the altitude above the ground, data quality of radiometric airborne data is strongly dependent on the flight heights. Also weather conditions and air radon concentrations (^{222}Rn) have a large impact on the data quality and can complicate the data processing. A complete overview (including theory, calibration, acquisition, processing and interpretation) about the gamma ray spectrometry method is given by the IAEA (2003).

[9] To emphasize that ^{238}U and ^{232}Th concentrations are not directly measured, finally determined uranium and thorium concentrations are presented in "eU" and "eTh" . The prefix "e" stands for "equivalent" or "effective".

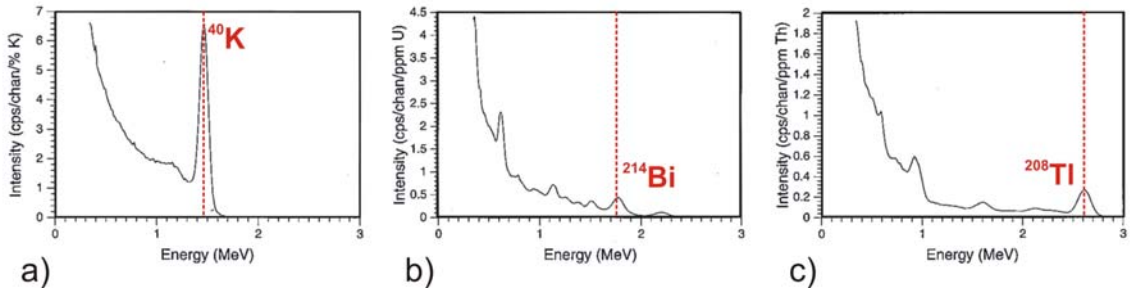

Figure A- 1: Simulated a) potassium-, b) uranium- and c) thorium spektra 100m above the surface. Red lines indicate ^{40}K, ^{214}Bi og ^{208}Tl maxima. Modified after Minty, 1997.

Appendix B: Characteristics of the EM system

Frequency label	Frequency in Hz	Coil orientation in m	Coil separation in m
F1	7001	Coaxial	6.27
F2	6606	H. Coplanar	6.27
F3	980	Coaxial	6.01
F4	880	H. Coplanar	6.01
F5	34133	H. Coplanar	4.90

Appendix C1: Flow chart of magnetic processing

Meaning of parameters is described in the referenced literature.

Processing flow:

1) Quality control and splitting of flight lines

2) Lag correction:

Used parameters:

Nr. of measured samples: 4

3a) Subtraction of a spiking and low-pass filtered version of the magnetic field of the base station:

Filters applied to the magnetic field of the base station:

-Non-linear low-pass filter (Naudy and Dreyer, 1968):

Used parameters:

Cut of wavelength: 120 samples

- Low-pass filtering:

Used parameters:

Cut of wavelength: 80 samples

3b) Adding a constant shift of 53400 nT.

5) Low-pass filtering:

Used parameters:

Cut of wavelength: 4 samples

5) Microlevelling with a median filter technique (Mauring and Kihle, 2006)

Used parameters:

Cut of wavelength of high pass filter:	400 m
Diameter of area to determine median values:	175 m
Length along profile to determine median values:	175 m

Appendix C2: Flow chart of EM processing

Meaning of parameters is described in the referenced literature.

Processing flow:

1) Quality control and splitting of flight lines

2) Lag correction:

Used parameters:

Nr. of measured samples: 4

3) Non-linear low-pass filter (Naudy and Dreyer, 1968):

Used parameters:

Cut of wavelength: 20 samples

4) Automatic drift correction

Several iteration of steps 5) and 6):

5) Manual reduction of residual drift

6) Inversion of inphase and quadrature data to calculate apparent resistivites. (Wait, 1987 and manual of the OASIS Montaj software "Geosoft")

7) Microlevelling with a median filter technique (Mauring and Kihle, 2006)

Used parameters:

Cut of wavelength of high pass filter:	400 m
Diameter of area to determine median values:	175 m
Length along profile to determine median values:	175 m

Appendix C3: Flow chart of radiometry processing

Underlined processing stages are not only applied to the K, U and Th window, but also to the total count window. Meaning of parameters is described in the referenced literature.

Processing flow:

1) Quality control and splitting of flight lines

2) Noise reduction with clustered NASVD (Minty and McFadden, 1998)

Used parameters:

Nr. of clusters:	80
Nr. of used EVs:	4

3) Life time correction (IAEA, 2003)

4) Airborne and cosmic correction (IAEA, 2003)

Used parameters (determined by high altitude calibration flights):

Aircraft background counts:

K window	10
U window	3
Th window	3
Total counts	150

Cosmic background counts (normalized to unit counts in the cosmic window):

K window	0.039
U window	0.029
Th window	0.034
Total counts	0.68

5) Stripping correction (IAEA, 2003)

Used parameters (determined from measurements on calibrations pads at the NGU):

a	0.0693
alpha	0.3126
beta	0.5121
gamma	0.7526

6a) Radon correction with spectral ratio method (Minty, 1998)

Used parameters (determined with the heuristic approach in Minty, 1998):

c1:	1.4
c2:	-1.949
c3:	0.744
c4:	-0.125

6b) Total count window was corrected for radon by making a correlation analysis of total counts and radon counts

Used parameter:

Nr. of removed total counts per Rn radon count in uranium window: 12

7) Height and topographic correction (Schwarz et al., 1992) to a height of 60 m

Used parameters (derived from Rønning, 2003):

Attenuation factors in 1/m:

K:	0.008
U:	0.006
Th:	0.006
Total counts:	0.0066

8) Microlevelling with a median filter technique (Mauring and Kihle, 2006)

Used parameters:

Cut of wavelength of high pass filter:	400 m
Diameter of area to determine median values:	175 m
Length along profile to determine median values:	175 m

9) Convert counts at 60 m heights to element concentration on the ground

Used parameters (derived from Rønning, 2003):

Counts per elements concentrations:

K:	83.8 counts/%
U:	7.11 counts/ppm
Th:	3.95 counts/ppm

Appendix D: Produced and delivered maps

Down-scaled image of maps originally produced in 1: 25 000

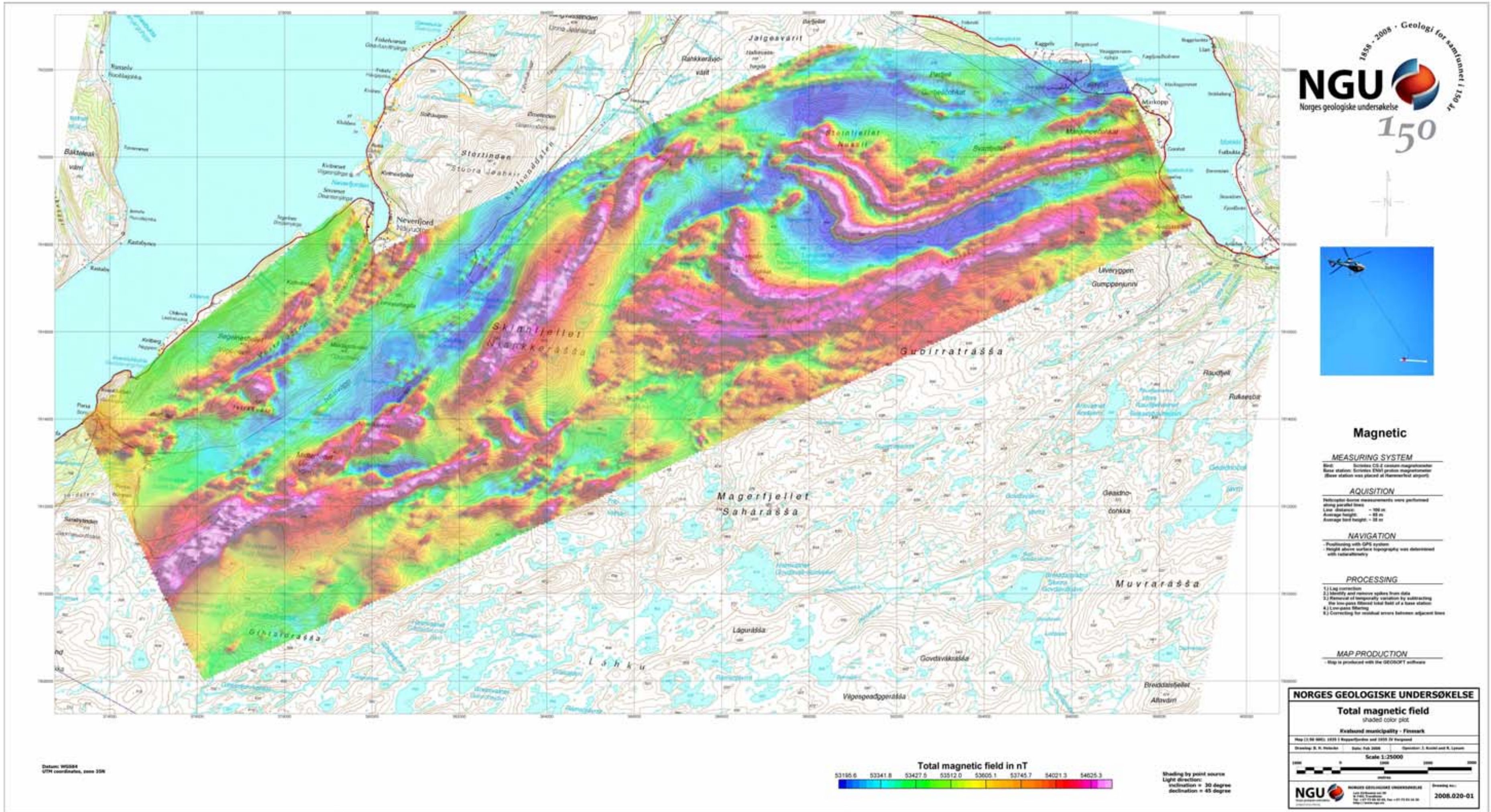

Figure D- 1: Magnetic total field. Map number 2008.020-01.

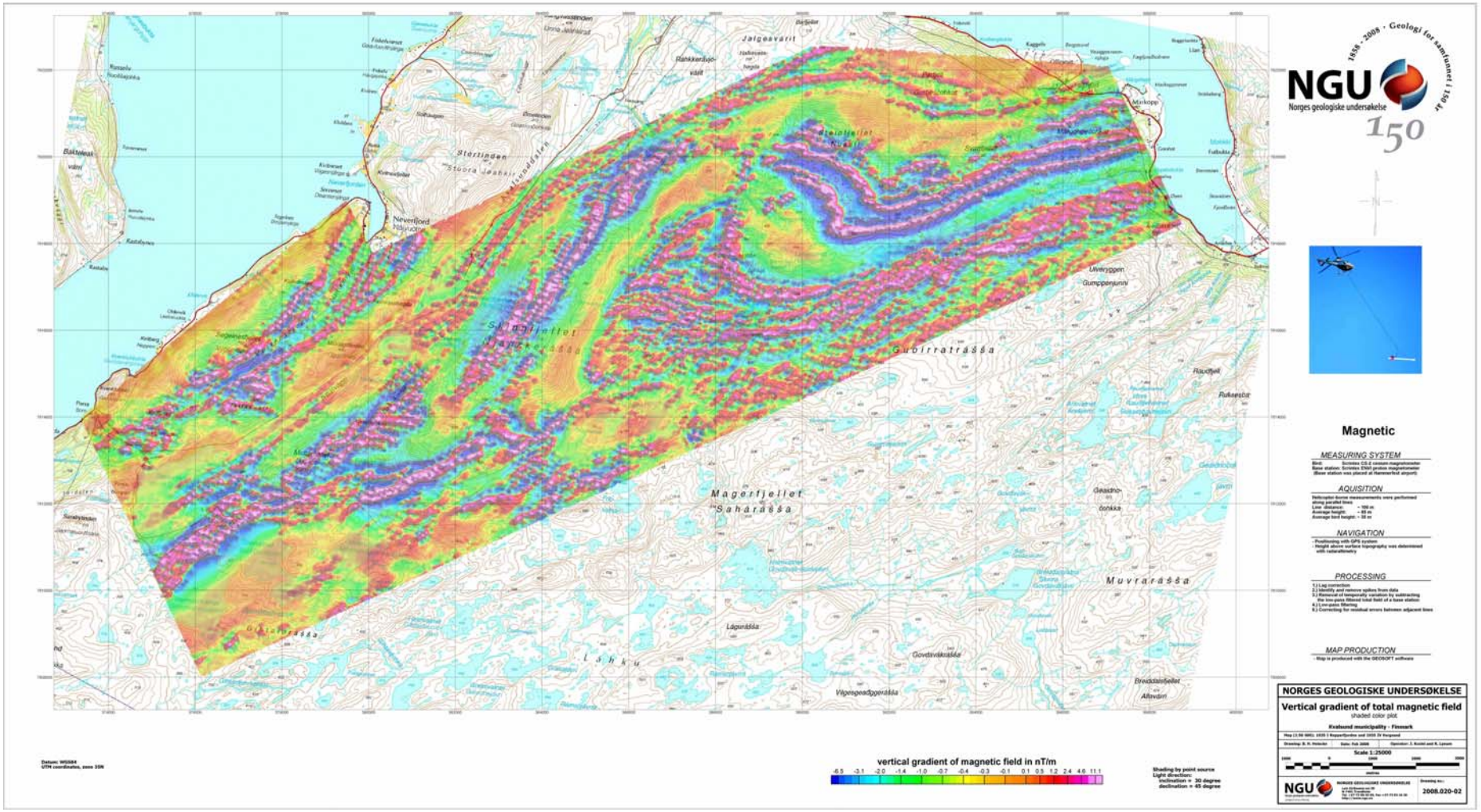

Figure D- 2: Vertical gradient of magnetic total field. Map number: 2008.020-02.

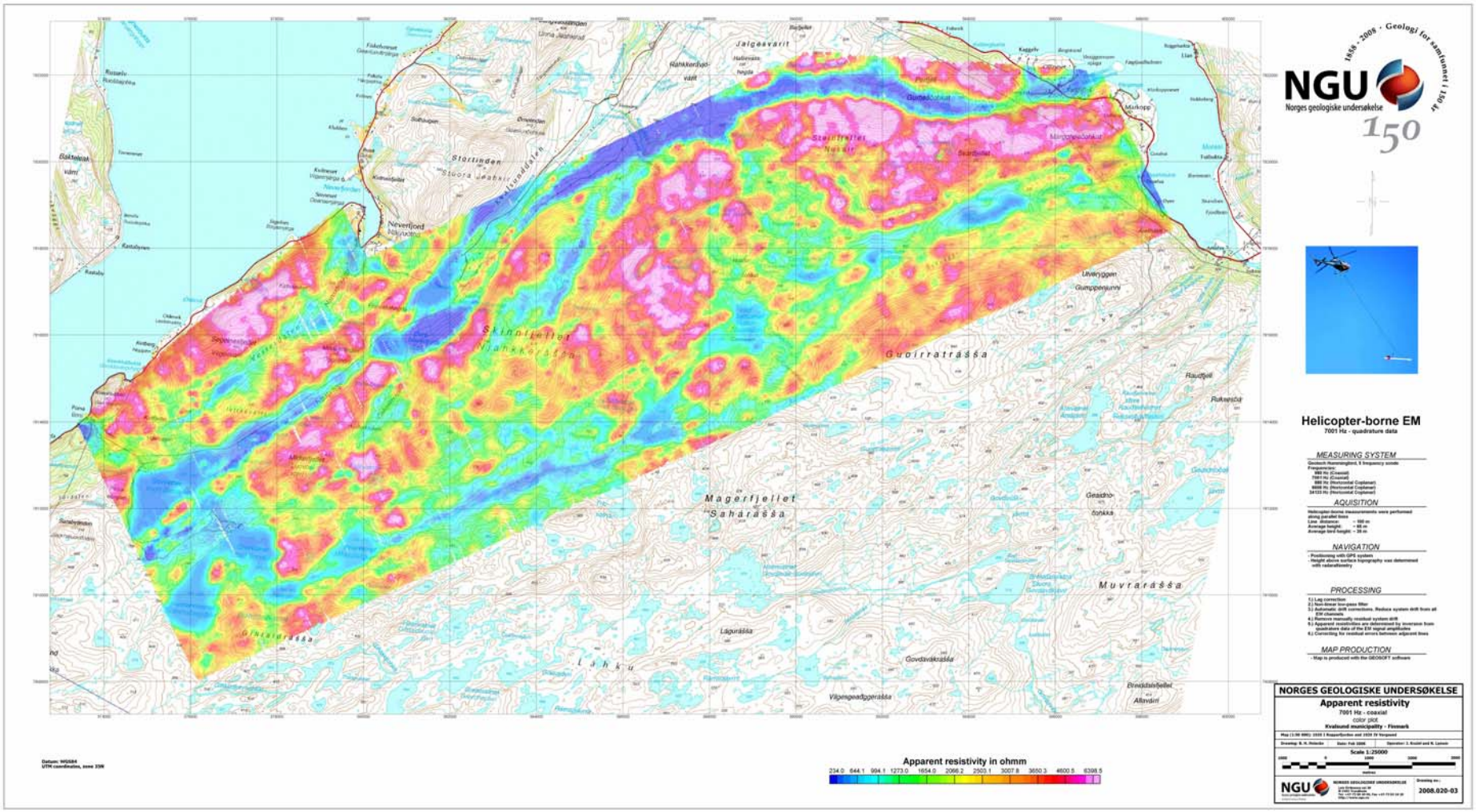

Figure D- 3: EM resistivity obtained from 7001 Hz (coaxial) quadrature data. Map number: 2008.020-03.

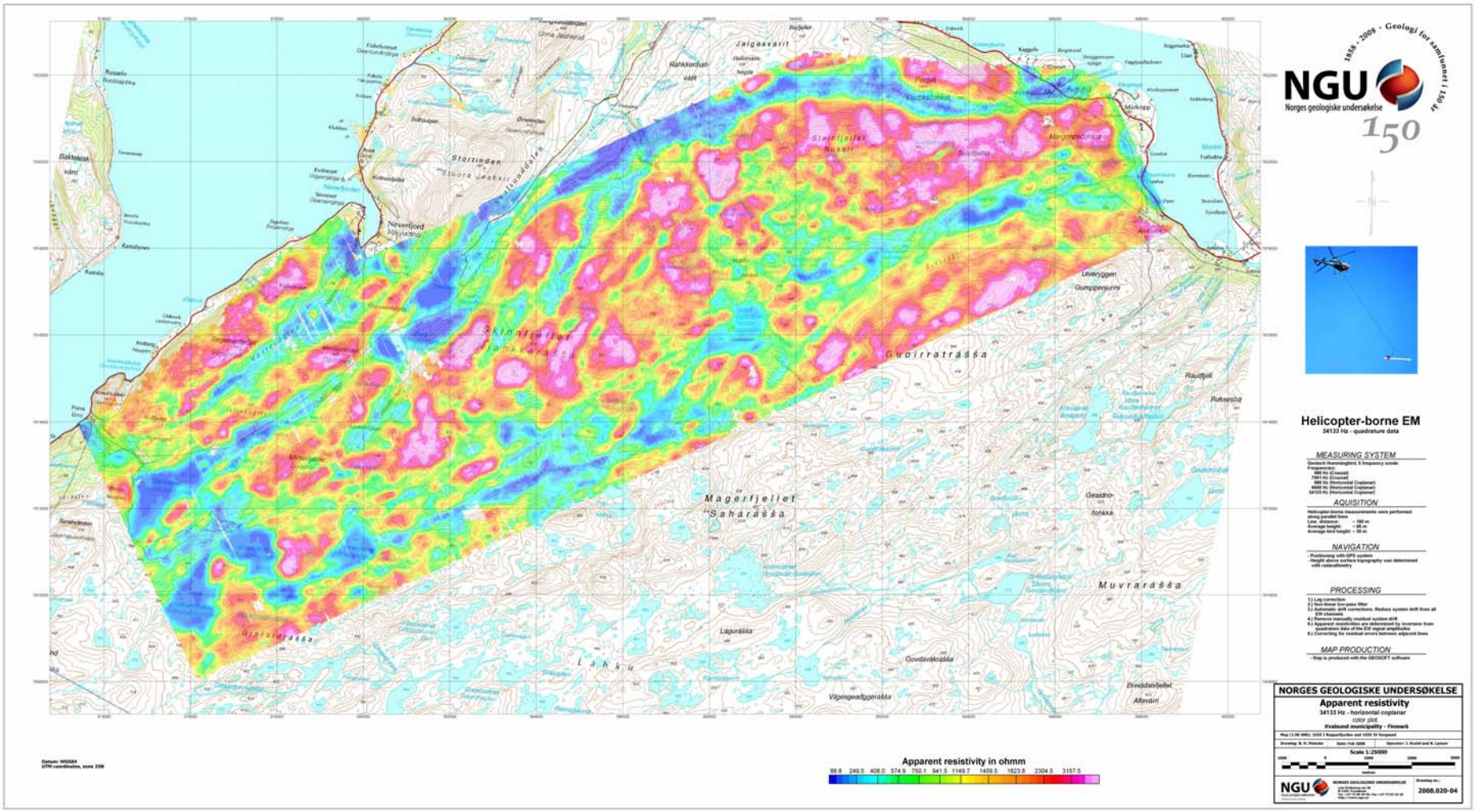

Figure D- 4: EM resistivity obtained from 34133 Hz (horizontal coplanar) quadrature data. Map number: 2008.020-04.

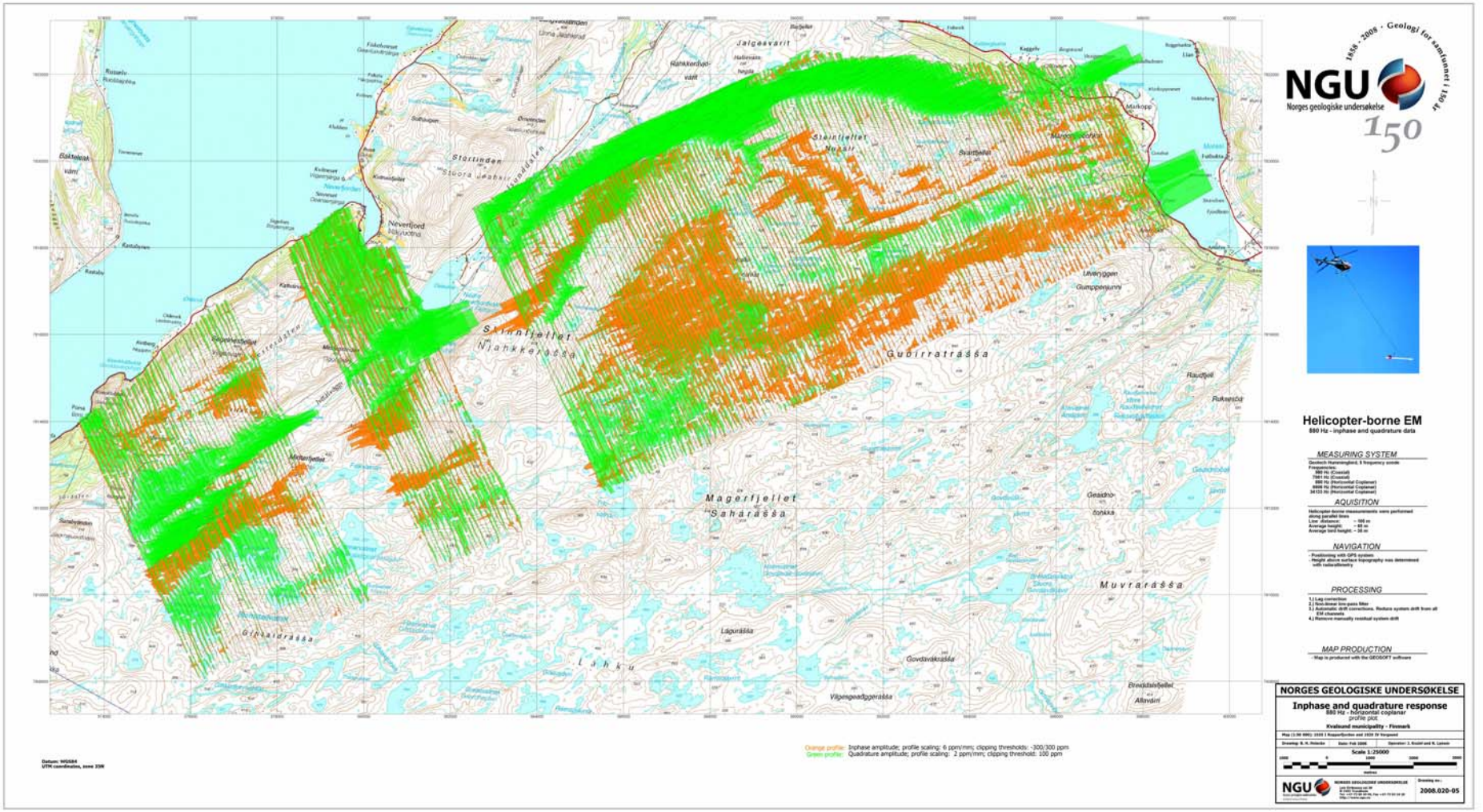

Figure D- 5: Profile plots of EM data (880 Hz, horizontal coplanar). Orange/(green) colors show the negative part of the inphase data /(positive part of the quadrature data). Map number: 2008.020-05.

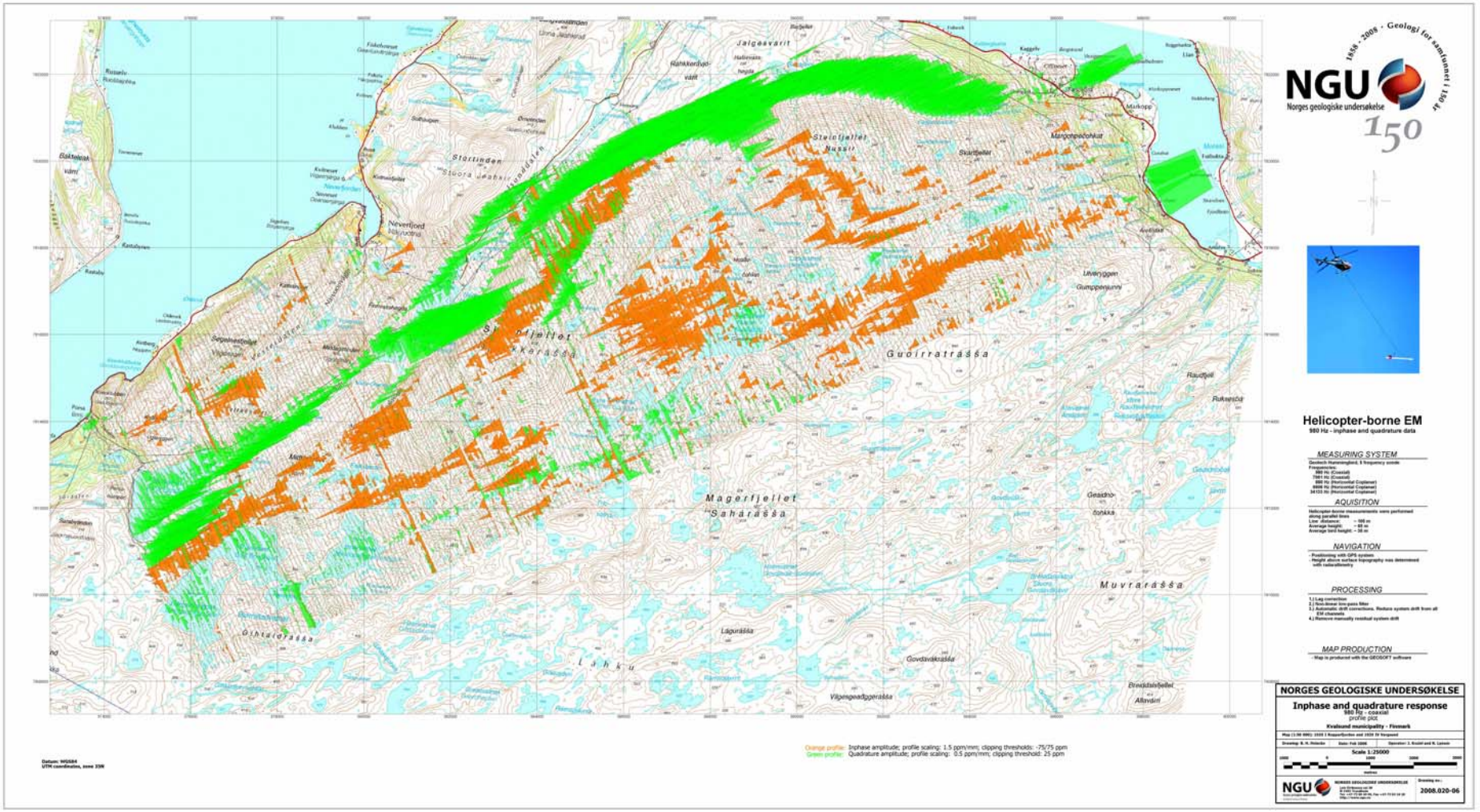

Figure D- 6: Profile plots of EM data (980 Hz, coaxial). Orange/(green) colors show the negative part of the inphase data /(positive part of the quadrature data). Map number: 2008.020-06.

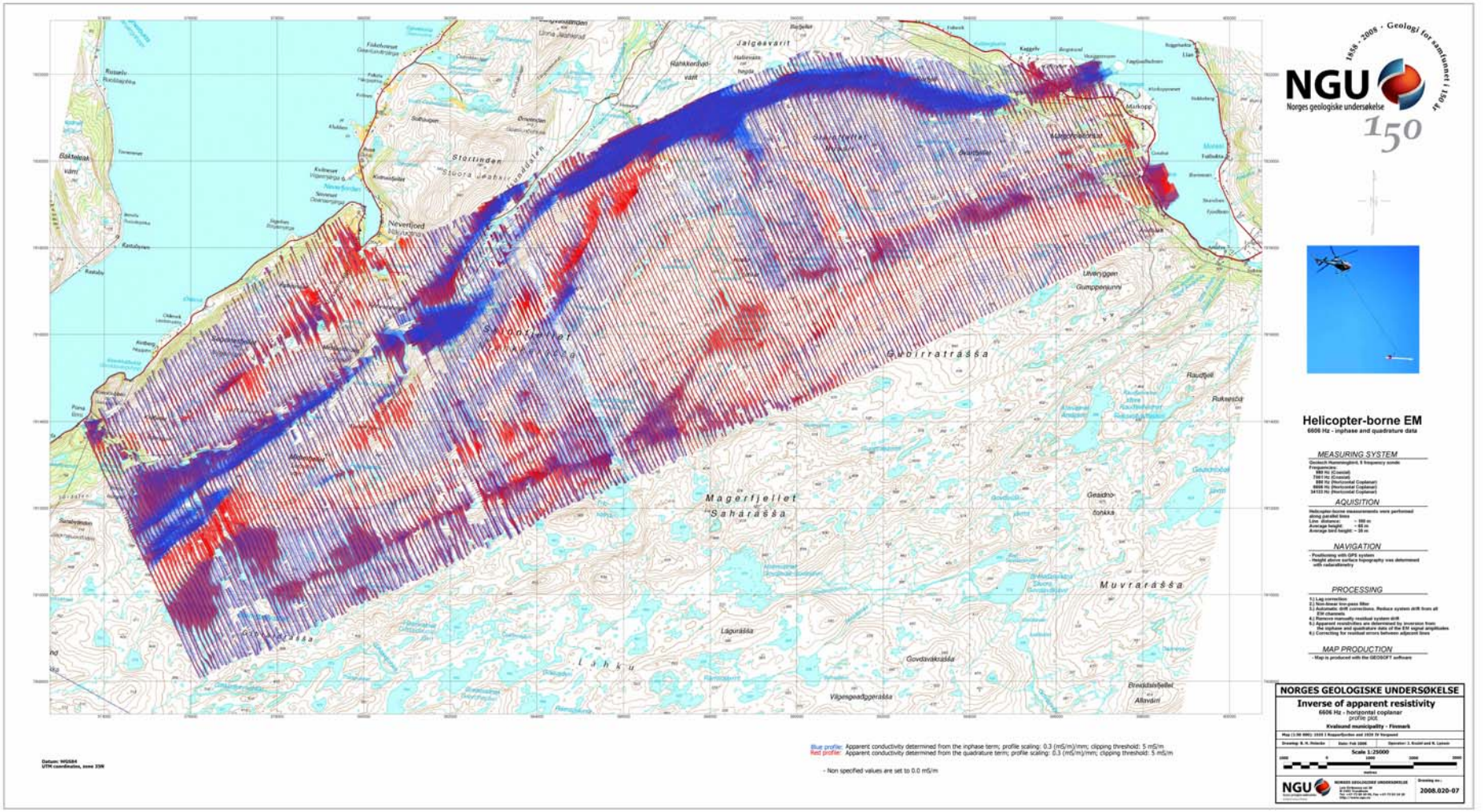

Figure D- 7: Profile plots of EM data (6606 Hz, horizontal coplanar). Blue/red colors show the conductivity obtained from the inphase/quadrature data. Map number: 2008.020-07.

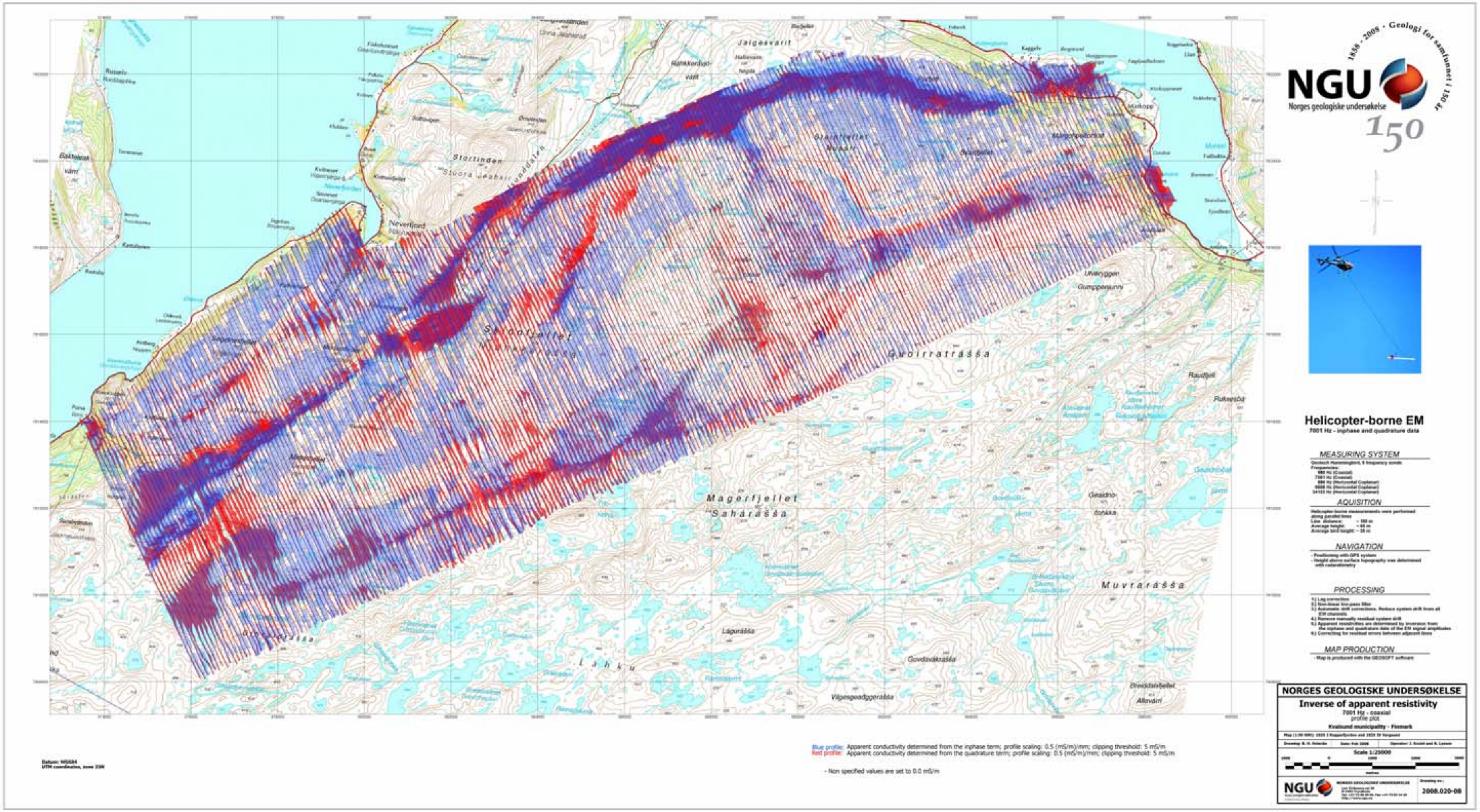

Figure D- 8: Profile plots of EM data (7001 Hz, coaxial). Blue/red colors show the conductivity obtained from the inphase/quadrature data. Map number: 2008.020-08.

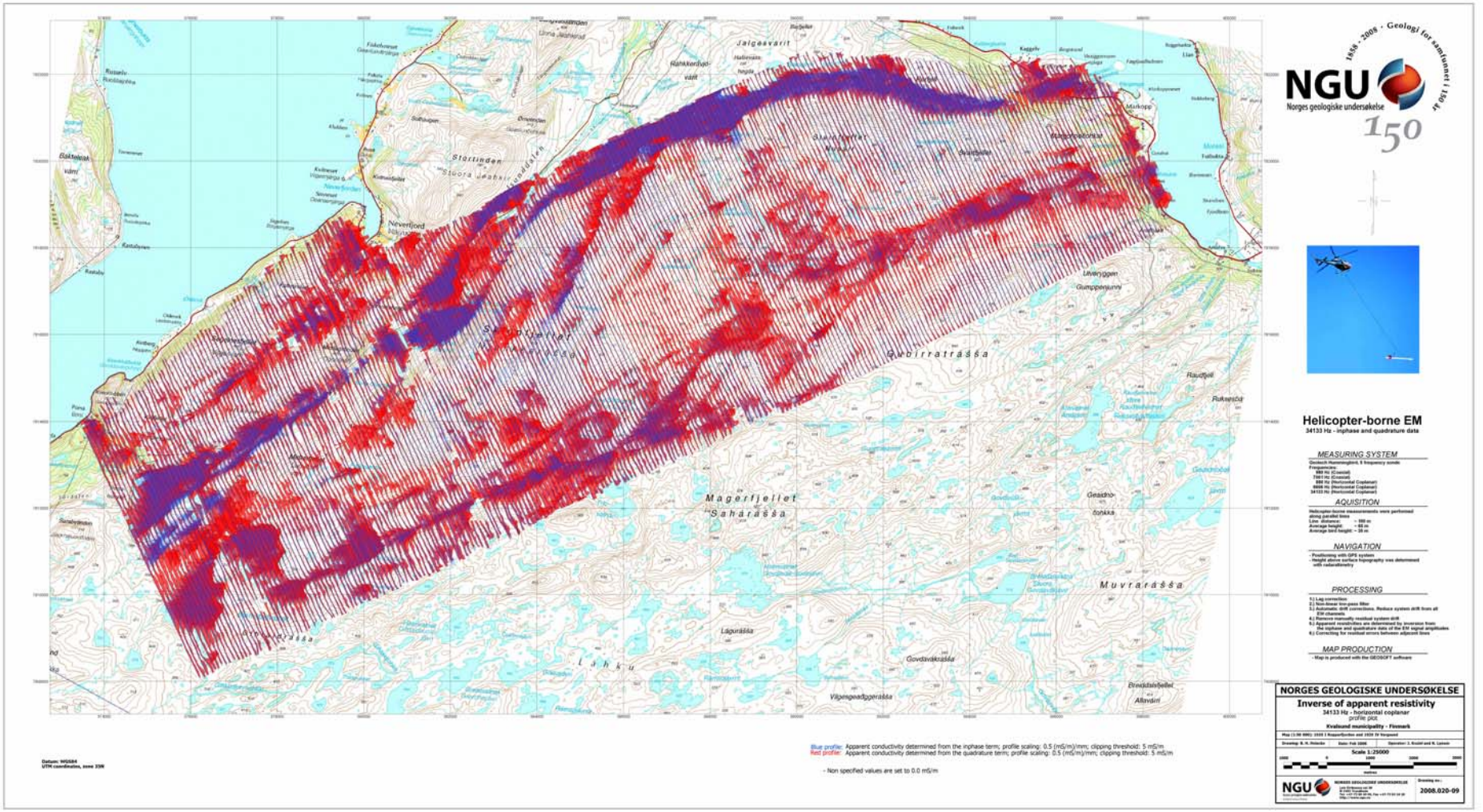

Figure D- 9: Profile plots of EM data (34133 Hz, horizontal coplanar). Blue/red colors show the conductivity obtained from the inphase/quadrature data. Map number: 2008.020-09.

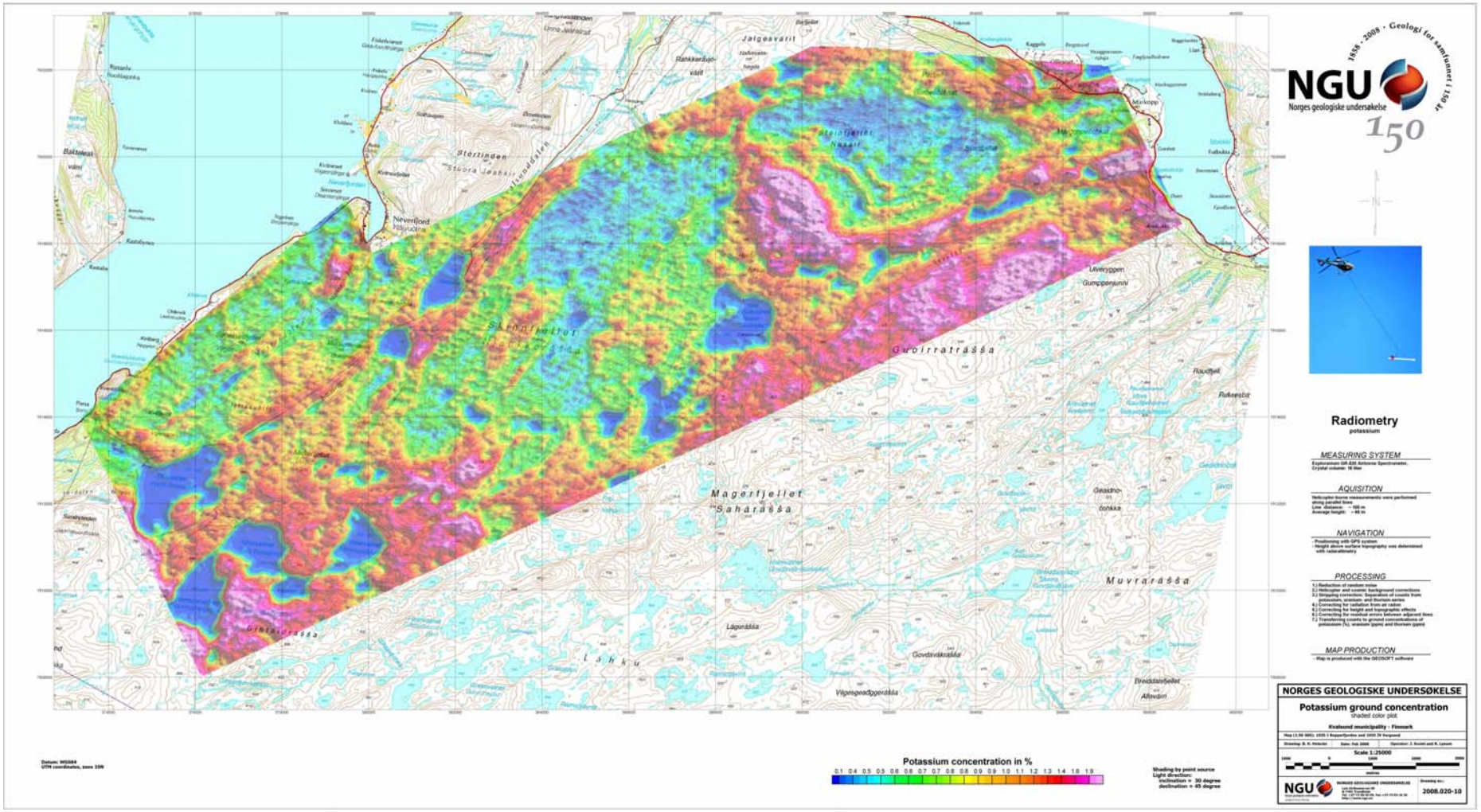

Figure D- 10: Radiometric potassium concentration. Map number: 2008.020-10.

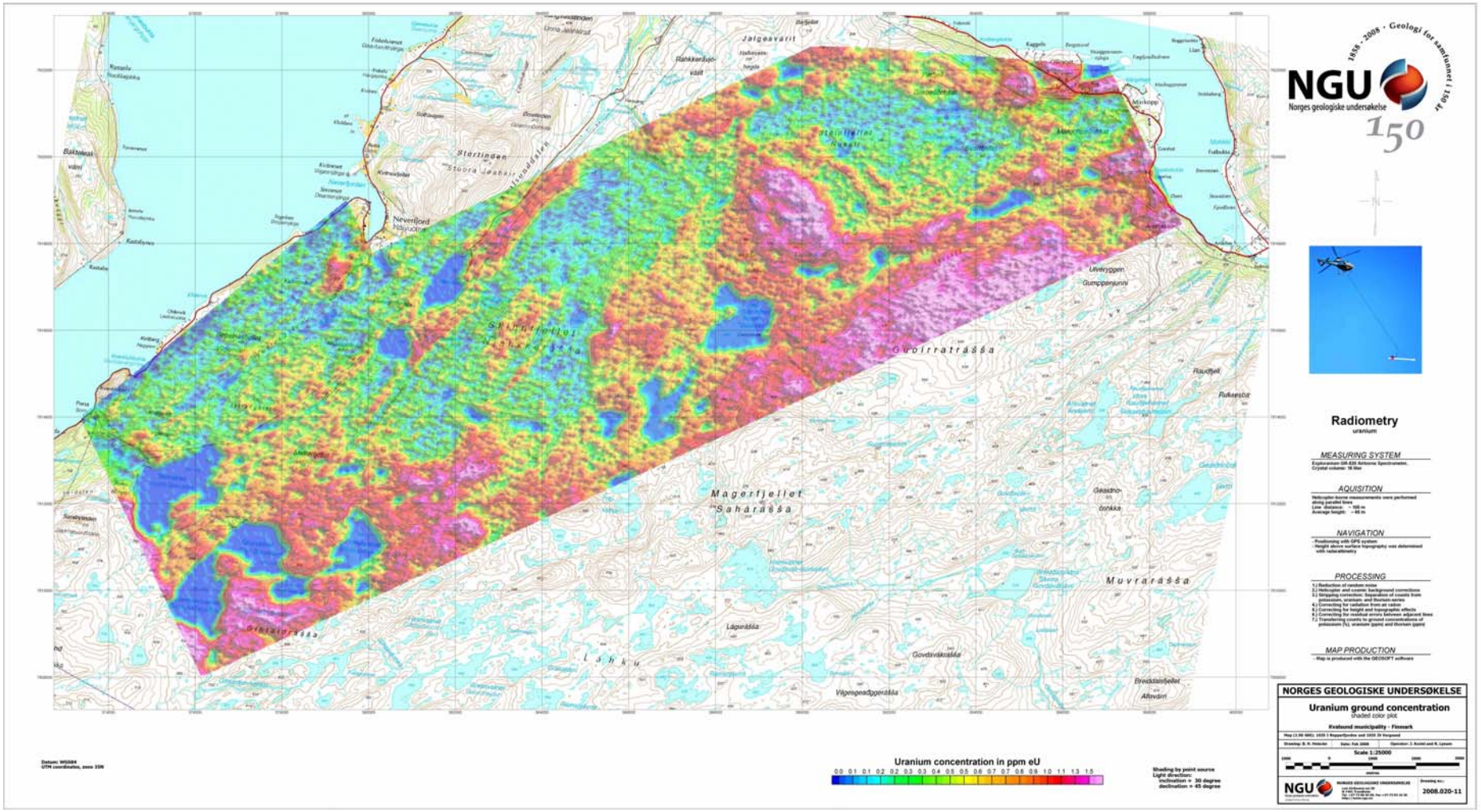

Figure D- 11: Radiometric equivalent uranium concentration. Map number: 2008.020-11.

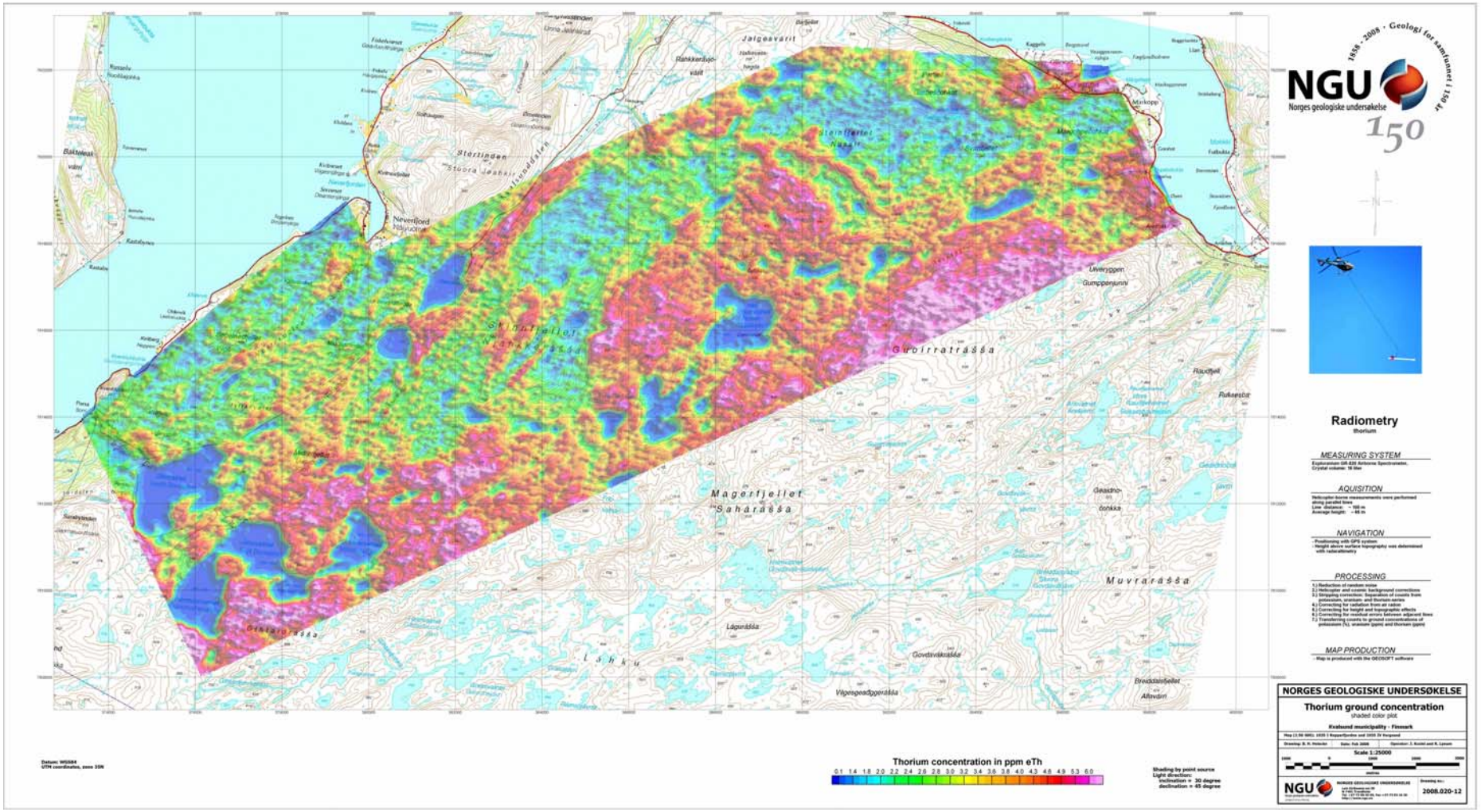

Figure D- 12: Radiometric equivalent thorium concentration. Map number: 2008.020-12.

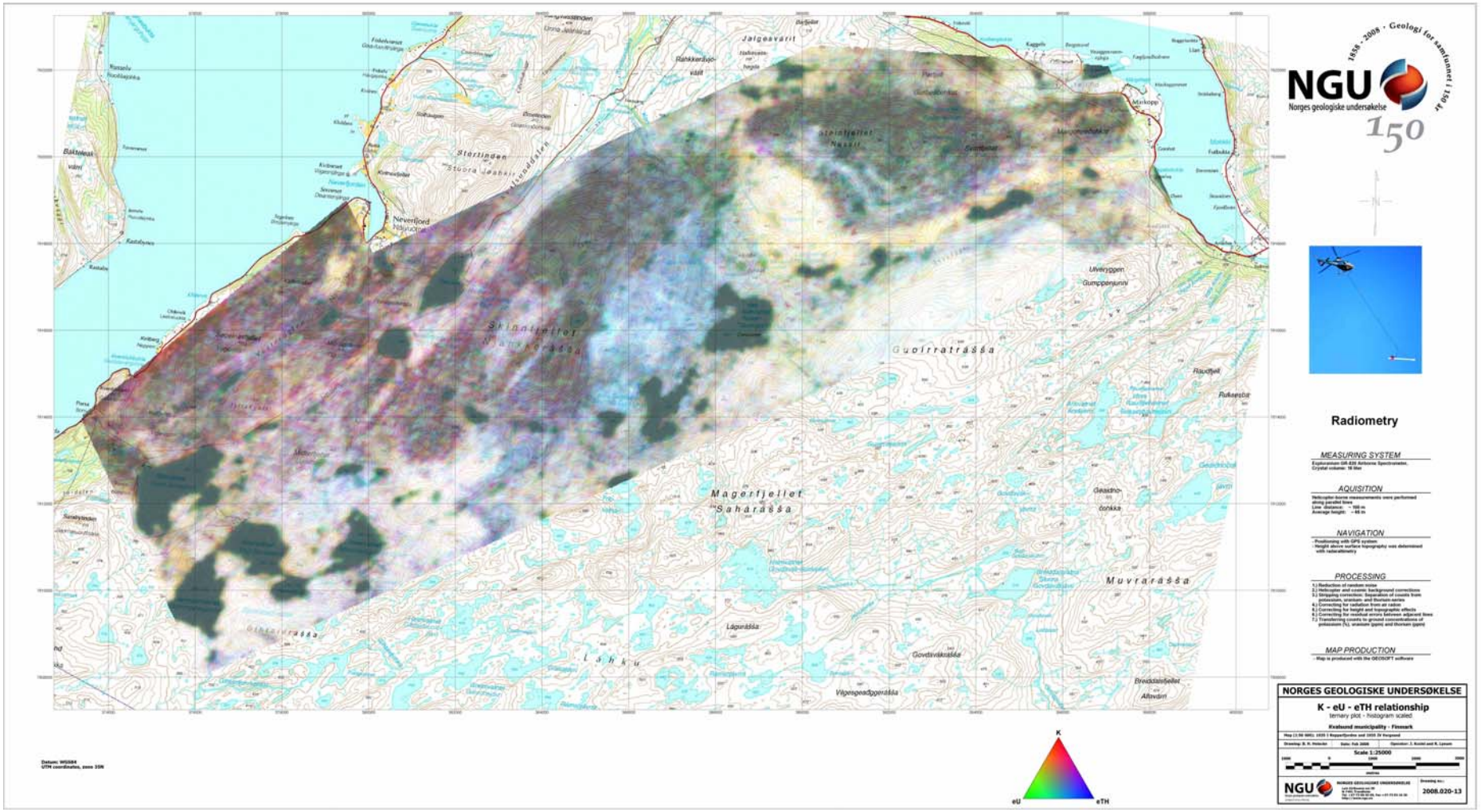

Figure D- 13: Ternary plot of the radiometric data. RGB color coding (red = K, green = eU, blue = eTh). Color scaling is histogram equalized. Map number: 2008.020-13

Norges geologiske undersøkelse
Postboks 6315, Sluppen
7491 Trondheim, Norge

Besøksadresse
Leiv Eirikssons vei 39, 7040 Trondheim

Telefon 73 90 40 00
Telefax 73 92 16 20
E-post ngu@ngu.no
Nettside www.ngu.no

Geological Survey of Norway
PO Box 6315, Sluppen
7491 Trondheim, Norway

Visitor address
Leiv Eirikssons vei 39, 7040 Trondheim

Tel (+ 47) 73 90 40 00
Fax (+ 47) 73 92 16 20
E-mail ngu@ngu.no
Web www.ngu.no/en-gb/